Universidade de Aveiro Departamento de Química
Ano 2018

Liliana Raquel Coelho Sousa

3D Bioprinting in liquid medium for the bioengineering of hybrid structures for regeneration of human tissues

Bioimpressão 3D em meio líquido para a bioengenharia de estruturas híbridas para regeneração de tecidos humanos

Universidade de Aveiro Departamento de Química
Ano 2018

Liliana Raquel Coelho Sousa

3D Bioprinting in liquid medium for the bioengineering of hybrid structures for regeneration of human tissues

Tese apresentada à Universidade de Aveiro para cumprimento dos requisitos necessários à obtenção do grau de Mestre em Biotecnologia Molecular, realizada sob a orientação científica do Professor Doutor João Mano, Professor Catedrático do Departamento de Química da Universidade de Aveiro e do Professor Doutor José Martinho Oliveira, Professor da Escola Superior Aveiro Norte da Universidade de Aveiro

Aos meus Queridos Pais e Avós

Por seu profundo amor, apoio e encorajamento

o júri

presidente

Doutor Jorge Manuel Alexandre Saraiva
Investigador auxiliar do Departamento de Química da Universidade de Aveiro

Doutora Carmen Sofia da Rocha Freire Barros
Investigadora principal do Departamento de Química da Universidade de Aveiro

Prof. Doutor João Filipe Colardelle da Luz Mano
Professor catedrático do Departamento de Química da Universidade de Aveiro

Agradecimentos

Em primeiro lugar gostaria de expressar a minha maior gratidão ao Professor João Mano pela oportunidade de realizar este projeto no seu grupo de pesquisa (COMPASS). Foi um grande desafio, mas ao mesmo tempo um prazer desenvolver este trabalho. Obrigada por me ter proporcionado acesso a todas as atividades das quais o grupo participou, e acima de tudo obrigada pela orientação e ajuda durante este percurso.

Um agradecimento também ao meu co-orientador Professor Martinho Oliveira por me ter acolhido tão bem na ESAN, pelo seu apoio, disponibilidade e contributo para a realização deste trabalho.

Um grande obrigado à Dra. Sónia Patrício, pela orientação, apoio e disponibilidade ao longo deste percurso. Obrigada por não ter desistido de mim e me ter feito evoluir tanto, não só a nível profissional, mas também a nível pessoal. Obrigada por todos os conselhos e por toda a amizade!

Agradeço também a todos elementos da ESAN por toda a simpatia demonstrada durante estes meses. De forma especial agradeço à Liliana Pires e ao Jorge Luís por toda a disponibilidade que mostram desde o início para participarem neste projeto, por toda a paciência, por toda a dedicação, por todos os conselhos, por todo o carinho. Sem vocês nada disto teria sido possível!

Também sou grata a todos os membros do COMPASS pelo companheirismo, pela amizade e pelo auxílio prestado durante estes últimos meses. Um especial obrigado ao Dr. Tiago Correia pela orientação no laboratório de biologia celular e ao Dr. Vitor Gaspar pela aquisição das imagens de fluorescência no confocal. E claro, obrigada a todos que iniciaram este percurso comigo, em especial à Mafalda, à Cátia e ao Bruno por terem tornado melhor o dia-a-dia no laboratório. Obrigada à Sara Santos por todos as conversas, conselhos e apoio! Serão certamente pessoas que levarei para toda a vida.

Agradeço a todos os meus amigos desde o Bacharelado em Bioengenharia aos Mestres em Biotecnologia e aos meus amigos desde sempre. Obrigada à Soraia, ao Luís, à Ana, ao Rui, à Sofia, ao Jó, ao João, ao Francisco, ao Vasco, que durante todos estes meses ouviram as minhas lamentações e me incentivaram a continuar. Obrigada por terem suportado todas as minhas ausências! Obrigada a todos aqueles que sempre tiveram uma palavra de carinho e incentivo o meu muito obrigado!

Agradeço ao Filipe Rocha pelo grande apoio e compreensão ao longo de todo este tempo e por nunca ter duvidado das minhas capacidades e me incentivado sempre a lutar pelos meus objetivos!

O meu maior obrigado vai para as pessoas mais importantes da minha vida, os meus pais e os meus avós por estarem presentes em todos os momentos da minha vida. Este trabalho não seria ser possível sem o seu amor, sem as palavras de incentivo que me fizeram por muitas vezes reerguer e eu agradeço profundamente todos os sacrifícios que fizeram para que esta experiência fosse possível. O vosso apoio e a vossa ajuda são e continuarão a ser fundamentais para mim!

palavras-chave Engenharia de tecidos; Impressão 3D; hidrogéis; goma xantana.

resumo

A medicina regenerativa e a engenharia de tecidos surgiram como metodologias alternativas para a substituição de tecidos ou órgãos lesados. Esta nova abordagem combina o uso de materiais naturais ou sintéticos com células com o objetivo de produzir um tecido que possua a mesma estrutura e funcionalidade do original. Diferentes técnicas de bioimpressão têm sido usadas para produzir estruturas de hidrogel contendo células. No entanto, essas abordagens têm sido limitadas a estruturas 2D ou tridimensionais simples (3D), uma vez que o fabrico de estruturas de hidrogel mais complexas, tal como vasos sanguíneos com contornos ramificados, requere um banho de suporte de modo a evitar o colapso da estrutura durante o processo de impressão.

Este trabalho baseia-se no desenvolvimento de um banho com propriedades reológicas adequadas ao processamento de estruturas complexas de hidrogéis por impressão 3D camada a camada. Por outro lado, pretende-se ainda que esse mesmo banho possa ser fotoreticulável após a impressão das estruturas de modo a permitir que hidrogéis, reticulados por processos reversíveis, possam ser facilmente removidos do banho de hidrogel formando construções perfuradas, igualmente atrativas para a regeneração de tecidos e órgãos uma vez que asseguram o transporte controlado de nutrientes e oxigénio.

A goma xantana possui excelentes propriedades reológicas, é biocompatível e de fácil modificação química pela diversidade de grupos funcionais que apresenta. Assim sendo, procedeu-se à impressão 3D de estruturas assimétricas complexas à base de hidrogéis de alginato em solução viscosa de goma xantana. O alginato reticulava rapidamente no banho de goma xantana pela presença do cloreto de cálcio, conseguindo depositar-se camada a camada sem provocar o arrastamento das camadas inferiores, colapsar ou dispersar no banho. Após impressão, conseguiu-se ainda retirar uma artéria com ramos assimétricos e injetar solução corada em cada uma das ramificações, demonstrando o fabrico bem-sucedido de uma rede ramificada complexa e perfurada. Avaliou-se ainda a biocompatibilidade do banho imprimindo filamentos de alginato com células do tipo L929, observando-se, após 7 dias em cultura, elevada viabilidade celular com formação de agregados de células.

Para a formação de um banho de hidrogel, procedeu-me à modificação química da goma xantana incorporando na cadeia polimérica secundária grupos metacrílicos, fotopolimerizáveis por ação da luz UV. A impressão 3D de um filamento de alginato tortuoso num banho de goma xantana metacrilada seguido do processo de fotoreticulação do banho comprovou a possibilidade de combinar 2 hidrógeis num só dispositivo. Além disso, a remoção do hidrogel de alginato por lavagem com EDTA demonstrou a elevada estabilidade química e estrutural do hidrogel à base de goma xantana para a formação de dispositivos perfurados. Em suma, desenvolveu-se com sucesso um banho biocompatível e de fácil processamento para processos de impressão 3D direcionados para uma variabilidade de aplicações biomédicas.

keywords Tissue engineering; 3D printing; hydrogels; xanthan gum;

abstract

Regenerative medicine and tissue engineering have emerged as alternative methodologies for the replacement of injured tissues or organs. This new approach combines the use of natural or synthetic materials with cells in order to produce a fabric that has the same structure and functionality as the original. Different bioprinting techniques have been used to produce hydrogel structures containing cells. However, such approaches have been limited to simple 2D or three-dimensional structures (3D), since the manufacture of more complex hydrogel structures, such as branched-out blood vessels, requires a support bath in order to prevent collapse of the during the printing process.

This work is based on the development of a bath with rheological properties suitable for the processing of complex hydrogel structures by 3D layer-by-layer printing. On the other hand, it is also intended that this the same bath can be photo-cross-linked after printing of the structures so that hydrogels, cross-linked by reversible processes, can be easily removed from the hydrogel bath to form perforated constructions equally attractive for the regeneration of tissues and organs since they ensure controlled transport of nutrients and oxygen.

Xanthan gum has excellent rheological properties, is biocompatible and easily chemically modified by the diversity of functional groups that it presents. Thus, 3D printing of complex asymmetric structures based on alginate hydrogels in viscous solution of xanthan gum was carried out. The alginate crosslinked rapidly in the xanthan gum bath by the presence of calcium chloride, getting deposited layer to layer without causing entrainment of the lower layers, collapsing or dispersing in the bath. After printing, we were able to remove an artery with asymmetric branches and inject colored solution in each of the branches, demonstrating the successful manufacture of a complex and perforated branched network. It was also evaluated the biocompatibility of the bath by printing alginate filaments with L929 cells, after which, after 7 days in culture, high cell viability with formation of cell aggregates was observed.

For the formation of a hydrogel bath, I proceeded to the chemical modification of xanthan gum incorporating in the secondary polymer chain methacrylic groups, photopolymerizable by the action of UV light. 3D printing of a tortuous alginate filament in a methacrylated xanthan gum bath followed by the bath photoreticulation process proved the possibility of combining 2 hydrogels in a single device. In addition, removal of the alginate hydrogel by EDTA lavage demonstrated the high chemical and structural stability of the xanthan gum hydrogel for the formation of perforated devices. In short, a biocompatible and easy-to-process bath has been developed successfully for 3D printing processes aimed at a variability of biomedical applications.

Contents

List of figures

List of tables

List of abbreviations

#

2D: two-dimensional

3D: three-dimensional

A

ALG: alginate

ALP: alkaline phosphatase activity

AM: additive manufacturing

B

DMSO: dimethyl sulfoxide

C

CAD: computer aided design

CAF: cancer- associated fibroblasts

CDLP: continuous direct laser deposition

CLSM: confocal laser scanning microscopy

D

DED: direct energy deposition

DLP: direct light processing

DMLM: direct laser deposition

DOD: drop-on-demand

E

ECM: extracellular matrix

EBM: electron beam fusion

EGF: epidermal growth factor

F

FBS: fetal bovine serum

FDA: food and drug administration

FDM: fused deposition modelling FRE: reversible forging reversible

H

HAECs: human aortic endothelial cells

I
iPSCs: pluripotent stem cells

L
LDH: lactate dehydrogenase
LENS: laser engineered net shape

M
MJF: multi jet fusion
MSC: mesenchymal stem cell

N
NPJ: nanoparticle jetting

P
PVA: photocrosslinkeble polyvinyl alcohol
PBF: power bed fusion
PDMS: polydimethylsiloxane
PEI: polyethylenimine
PVA: photocrosslinkeble polyvinyl alcohol

S
SHS: selective heat sintering
SLA: stereolithography
SLS: selective laser sintering
STL: standard triangle language

T
TE: tissue engineering

U
UV: ultraviolet

X
XG: xanthan gum

Chapter I

Background

1. Introduction

1.1 Additive Manufacturing

Additive manufacturing (AM), is a term that encompass many others such as 3D Printing, Rapid Prototyping, Rapid Manufacturing, Direct Digital Manufacturing or Layered Manufacturing. This technique is defined by ASTM F42 and ISO TC 261 as "a process of joining materials to make parts from 3D model data, usually layer upon layer, as opposed to subtractive manufacturing and formative manufacturing methodologies" [1].

Additive manufacturing technology first emerged in the 1980s and was used to create 3D solids by solidification of thin layers of UV light sensitive liquid polymer using a laser with a technique known as Stereolithography (SLA) [2]. Some years later was first introduced the first Fused Deposition Modelling (FDM) machine, a technology that extrudes plastic to deposit it forming layers on a print bed or over the previous layer [3,4]. Then, in 1992, the first SLA 3D printer machines were first produced over the patent and simultaneously also the first Selective Laser Sintering (SLS) machine. First wax printer was released in 1994, and after that, during the year 2000, the first 3D inkjet printer and first multicolour 3D printer were produced. In the last years many variations, subtypes and different technologies have emerged with different degree of success in the manufacturing industry however between this big amount of AM printers is probably, because of its implications in medicine science, the first biocompatible material FDM machine, which was produced in 2008 [3,5].

This method of fabrication has been widely used in engineering given their good accuracy and high reproducibility, also since we can obtain complex structures in less time. With these techniques it is still possible to produce tissues exactly in the format of those that replacement, and with biological characteristics appropriate to each patient [6]. This technique changing radically implantology and regenerative therapies by adding new possibilities to create tissues with multiple cell lines and organs [7, 8].

1.1.1. Additive Manufacturing process

The manufacturing process of additive layers always start in the same way. The first step is to create a computer aided design (CAD) model of the object to be printed. Subsequently the CAD file is then

converted to a standard additive file format - usually a Standard Triangle Language (STL) file, which uses triangles to describe the surfaces of an object. Converting to an STL file formats the forms and time required. This file is then imported into a slicer program, where it will be cut into several layers, depending on the precision you want [9] (figure 1.1).

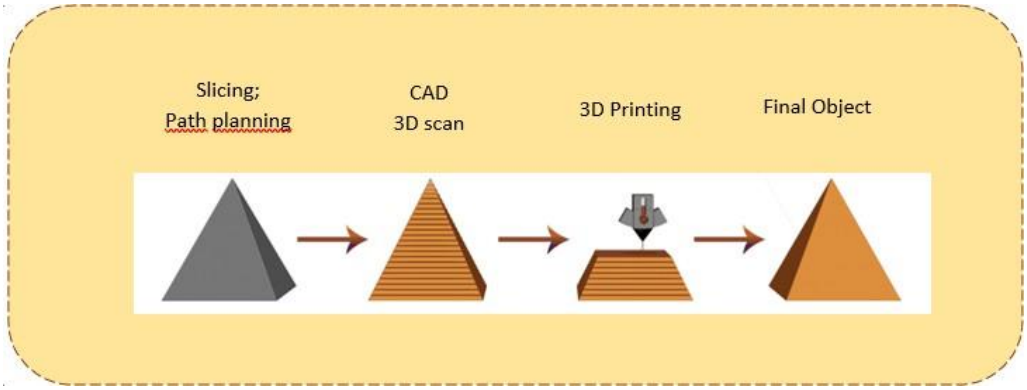

Figure 1.1. 3D printing works in 4 steps.

A wide range of different processes is available under the AM technique. AM manufacturers have created process names and unique material designations, although most different systems employ similar processes and share similar or identical materials. These processes are categorized using different criteria, from the application (visual prototyping, functional prototyping, fast tools and fast manufacturing) to the initial condition of processed materials or the physical principle underlying the process of solidification mainly in layers [10].

To meet the different requirements of the market, the industry currently relies on AM professional machines based on one of the seven major manufacturing processes, being Material Extrusion, Directed Energy Deposition, Material Jetting, Binder Jetting, Sheet Lamination, Vat Polymerization, Powder Bed Fusion [11]. In table 4.1 are described the basic principles, materials, advantages and disadvantages of these Additive Manufacturing categories.

Figure 1.2. Classification of Additive Manufacturing processes.

- **Material Jetting**

Material blasting is a process where droplets of building material are deposited selectively. Layers harden when they cool or are cured by ultraviolet light.

- **Binder Jetting**

Binder blasting is the process of dispensing a liquid binding agent onto a bed of powder to build up a portion of one layer at a time. These layers bond together to form a solid component.

- **Sheet Lamination**

The sheet lamination process is a process that uses sheets or metal ribbons, which are joined using ultrasonic welding to form an object.

- **Vat Polymerization**

Photopolymerization of vat occurs when a liquid photopolymer resin is exposed to light of a specific wavelength and undergoes a chemical reaction to become solid. Approaches to AM based on lithography and stereolithography (SLA) can be grouped into this category.

- **Power Bed Fusion**

Powder Bed Fusion (PBF) technology is an additive manufacturing process in which uses a heat source that induces the melting (sintering or melting) between the particles of a plastic or metal powder, one layer at a time, to produce a part there is a wide range of PBF technologies including direct laser sintering (DMLS), selective laser sintering (SLS), selective heat sintering (SHS), electron beam fusion (EBM) and direct laser fusion (DMLM).

- **Direct Energy Deposition (DED)**

Direct Energy Deposition creates parts using concentrated thermal energy (for example, an electric beam or a laser beam gun). This type of technology is used exclusively for metals and polymers.

- **Material extrusion**

Material extrusion is one of the most well-known additive manufacturing processes. It is a technique for depositing polymers, pastes and dispersions computer controlled, layer by layer, through a heated nozzle mounted on a movable arm. Adhesion between the layers occurs through the control of temperature or the use of chemical binding agents. The success and print properties of MEAM processes depend on processing parameters such as extrusion temperature, layer thickness, bed temperature and print speed. This process offers a reduction in the time and cost of manufacturing compared to other techniques and allows the creation of complex structures. These advantages led to the use of this technique in the aerospace industry, architecture and medicine.

It includes various techniques such as FDM, FFF, 3D dispensing, 3D micro extrusion, 3D microfiber extrusion, 3D fiber deposition, dosing and deposition of fluids and 3D plotting. These techniques cover the use of a wide range of materials. FDM uses thermoplastics, 3D extrusion uses rubbers, silicones, polyurethanes, biomaterials, hydrogels and even living cells [12].

Table 4.1. Basic principles, materials, advantages and disadvantages of seven ASTM categories of Additive Manufacturing. Adapted from Refs [13,11].

Process	Technique	Materials	Advantages	Disadvantages
Material Jetting	• Nanoparticle jetting (NPJ) • Drop-On-Demand (DOD)	Polymers Plastics	• Multiple material parts and colors under one process • Low waste	• Support material is often required
Binder Jetting	• Binder Jetting	Ceramics Metals Polymers	• Parts can be made with a range of different colors • Process Faster	• High post-processing time
Sheet Lamination		Paper Plastics Metals	• Process Faster • Low cost • Ease of material handling	• Require post processing to achieve desired effect
Vat Polymerization	• Direct Light Processing (DLP) • Continuous DLP (CDLP) • Stereolithography (SLA)	Resins Polymers	• High level of accuracy and good finish • Relatively quick process	• Requires support structure • Relatively expensive
Power Bed Fusion	• Selective Laser Sintering (SLS) • Selective Laser Melting (SLM) and Direct Metal Laser Sintering (DMLS) • Electron Beam Melting (EBM) • Multi Jet Fusion (MJF)	Plastics Metals Polymers	• Large range of material options • Relatively inexpensive • Ability to integrate technology into small scale	• Slow speed • Size limitations • High power usage
Direct Energy Deposition	• Electron Beam Additive Manufacture (EBAM) • Laser Engineered Net Shape (LENS)	Metals	• Ability to control the grain structure to a high degree	• Require post processing to achieve desired effect
Material Extrusion	• Fused Deposition Modeling (FDM)	Polymers Plastics	• Widespread and inexpensive process	• The nozzle radius limits and reduces the final quality • Constant pressure of material is required

Even though all technologies are different and based on distant physical principles, they all share the same philosophy of adding sequential layer material. This layer-by-layer manufacturing process is managed under automated control. The main considerations on the machine selection are the speed in printing, cost of the 3D printer, cost of each printed piece, cost and choice of materials, colour capacity, multi-material capacity, configuration possibilities, resolution and resistance and resistance part.

3D Printing have a lot of applications in a wide range of disciplines, varying from the medical world to the food industry, can be used to print electronic devices, ceramic and

glasses, artificial tissues and organs and automotive and aircraft components. As we have already seen 3D printing, we can use a wide range of materials ranging from plastics, resins, ceramics to biomaterials.

Among the groups presented above, there are 3 that are widely used in tissue and organ engineering: inkjet bioprinting, laser bioprinting, and extrusion-based bioprinting (figure 1.3).

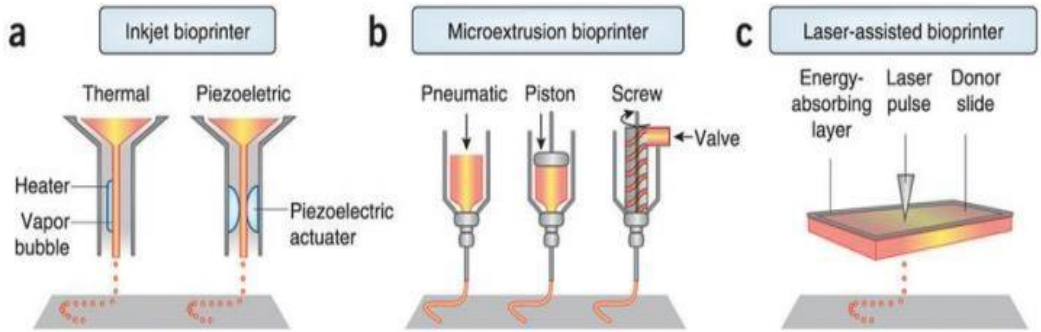

Figure 1.3. The different types of 3D bioprinting technologies for tissue and organ engineering: (a) inkjet-based bioprinting; (b) extrusion-based bioprinting; (c) laser-based bioprinting. Image from [14].

Among the developed bioprinting techniques, extrusion-based bioprinting (usually only called bioprinting) is one that provides greater structural integrity and is still capable of delivering a wide variety of biomaterials and cells including native and synthetic hydrogel polymers and cell aggregates while other techniques are limited to bioprinting hydrogel polymers with suspended cells [15,16].

This technique acts by extruding biomaterials through a nozzle, by means of a pressure assisted system, under the control of a robotic three-axis automated system. During the impression, the dispensing head is moved along X and Y axes controlled by the robotic system to deposit biomaterial/cell solutions onto a stage, and moved up or down along the Z axis to deposit different layers and form the scaffolds as directed by the CAD models [17,18].

Materials play a key role in tissue scaffold bioprinting, since they provide the physical support and structural interface required for cell and tissue interactions. A high understanding of the materials and their properties before printing is then necessary.

1.2. Tissue engineering and Regenerative medicine

Transplantation of tissues and organs currently represents a generally accepted treatment for the millions of patients who suffer from the loss or failure of tissues or organs due to accidents or illness. This conventional approach, however, presents some limitations, such as the long wait for donated organs and the serious complications of immunity that may arise [19]. Then tissue engineering emerges which may be the answer to overcome these obstacles.

Tissue engineering is one of the fields of regenerative medicine initially defined by Langer and Vacanti as "an interdisciplinary field that applies the principles of engineering and life sciences to develop biological substitutes, typically composed of biological and synthetic components that restore, maintain, or improve tissue function " [20]. This field of regenerative medicine is composed of three main components: cells, the supporting structure or scaffold and biomolecules or growth factors. The weighting and choice of each is decisive for the success of the construction after the implantation at the target location.

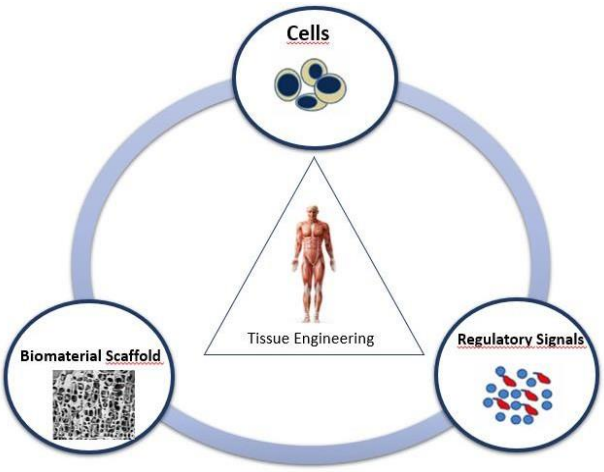

Figure 1.4. Tissue engineering triad of cells, signals and the scaffold which act as a template for tissue formation.

1.3. Bioinks

3D bioprinting is a technology to fabricate constructs from living cells with or without a carrier material in a layer-by-layer. The material that is printed is referred to as a "bioink," which can be defined as an ink formulation that allows printing of living cells. The ideal bioink formulation should satisfy certain material and biological requirements, such as bioprintability, high mechanical integrity and stability, insolubility in cell culture medium, biodegradability at a rate appropriate to the regenerating tissue, non-toxicity and nonimmunogenicity, and the ability to promote cell adhesion [21,22] (figure 1.5). Other relevant requirements are listed below:

-Biocompatibility: When within the body, the material should have a favourable response when in contact with the tissues, i.e. it must have minimal allergic, inflammatory or toxic reactions. However, the body always has a response to any foreign body inserted therein, which can be bypassed by changing some properties of the materials, thus mimicking the tissue response.

-**Biodegradability:** when in contact with organic fluids, the material degrades, causing soluble products, which are excreted by the metabolic mechanisms that the organism has, so it is not necessary to undergo surgical interventions to remove them [23].

-**Physical properties:** The carrier must possess adequate mechanical properties, ideally corresponding to those of the original tissue, which allow enough cell growth and maintenance of the appropriate extracellular matrix. In addition, some level of bioactivity must be provided by the scaffold surface to accommodate cell adhesion and migration [24].

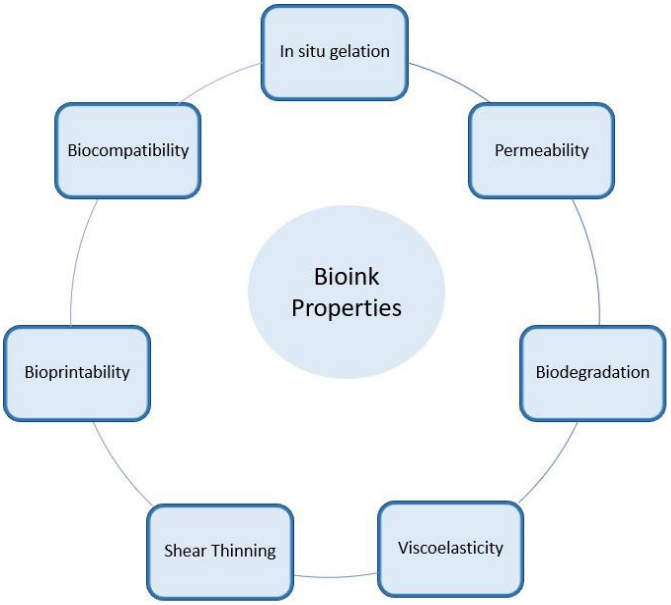

Figure 1.5. Bioinks properties.

There are many bioink materials used in 3D bioprinting processes including scaffold-based (hydrogels, microcarriers and decellularized matrix components), and scaffold-free (cell aggregates) bioink materials[25]. Scaffold based comprises the type of bioinks used in "Top Down" approach, where the scaffolds are seeded with cells after bioprinting and scaffold free comprises the bioinks used in a "Bottom up" approach, where highly hydrated polymers are combined with cells prior to bioprinting [26].

The scaffold-based bioprinting approach is the most widely used approach to date because it provides an area for cell adhesion and a biological cue for cell differentiation. There are three categories that encompass the scaffold-based bioinks: hydrogels, decellularized extracellular matrices and cell suspensions [27]. Due to their properties, hydrogels are the most used in tissue engineering [28].

1.3.1. Hydrogels

Hydrogels are hydrophilic three-dimensional networks with similar morphology to ECM. These matrices are insoluble in water due to the presence of chemical and/or physical crosslinking points. These materials are widely used in bioprinting since to their hydrophilic portions they provide fast gelling times and improved mechanical strength that can support 3D structures, it also provides a good homogeneous distribution of substrates and facilitate the diffusion of the molecular oxygen necessary for cellular

viability. Hydrogels are still capable of absorbing large amounts of water (99% w/w), and have low toxicity, which makes them good ECM mimics [29].

For any material, the physical, chemical and mechanical properties play an important role in determining if it is suitable for a given application. Hydrogels have a variety of properties including their absorption capacity, swelling behaviour, permeability, surface properties, optical properties and mechanical properties which make them promising materials for a wide variety of applications [30].

Also, the rheological properties of hydrogels have proved extremely important. A hydrogel exhibits a viscoelastic behaviour, that is, it behaves neither as purely viscous liquids nor as pure elastic solids, exhibiting a viscous component, consonant with "Lei de Newton" for viscosity and an elastic component in accordance with "Lei de Hooke" [31].

Given their properties, the use of hydrogels as biomaterials is currently a rapidly developing area. The history of hydrogels as biomaterials goes back to the 1960s, when Wichterle and Lim first prepared hydrogels of Hydroxyethyl Methacrylate (HEMA) [32]. Currently, there is a wide range of materials that can be used as the basis for a hydrogel for application as biomaterial.

Hydrogels are used in biofabrication and tissue engineering for a wide array of applications such as drug delivery [33], contact lenses [34] and wound dressings [35]. There are also many other applications such as absorbent materials, membranes, microcapsules, support for catalysts, breast implants, etc [36]. The most recent and exciting applications of hydrogels are cell-based therapeutics [37] and soft tissue engineering [38].

1.3.1.1. Classification of hydrogels

Hydrogels are classified into several categories: classification based on source, classification according to polymeric composition, classification based on configuration, classification based on type of cross-linking, classification based on physical appearance and classification according to network electrical charge. [39]

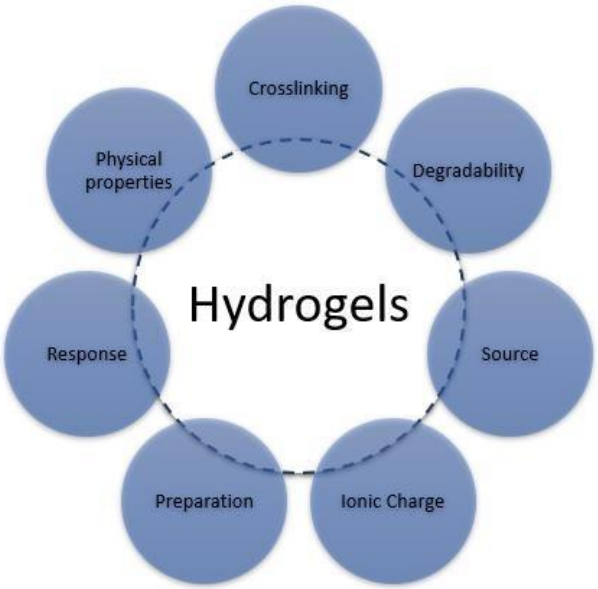

Figure 1.6. Classification of hydrogels based on different parameters. Addapted from Ullah, F., et al. [40]

Based on source hydrogels can be classified into two distinct categories, the natural and the synthetic hydrogels.

Synthetic polymers have predictable and reproducible physical and mechanical properties as result of controlled conditions during synthesis. An important advantage offered by this class of polymers is a high impurities control over the natural polymers. Thus, it diminishes any possible risks of toxicity or immunogenicity. Synthetic hydrogels also offer more flexibility to adjust chemical composition and mechanical properties. Among the various known synthetic hydrogels, the most used are poly (ethylene glycol) diacrylate, poly (acryl amide), poly (vinyl alcohol) [41,42].

Natural hydrogels include collagen, fibrin, hyaluronic acid, matrigel and derivatives of natural materials such as chitosan, alginate, cellulose and agarose. Natural polymers are preferred to synthetic polymers because of cell affinity and similarity to ECM, however they do have some disadvantages, such as the fact that polymerization or gelling conditions are often poorly understood and because of their natural origin, their composition may vary from one lot to another [43,44]. Natural hydrogels have been widely used for stem cell culture and regulation because of their desirable properties such as biocompatibility and biodegradability [45].

Of all the polysaccharides, a greater incidence is observed in the use of Alginates, material coming from the brown algae, due to its reversible gelation (ionic crosslinking) and the high biocompatibility. However, this material presents a disadvantage, since it is

easily degraded by loss of the divalent ions, which, during the preparation of the solution, are solubilized in the aqueous medium.

Alginates (ALG) are a group of naturally occurring anionic and hydrophilic polysaccharides obtained from many species of brown seaweed cell walls, including *Macrocystis pyrifera*, *Laminaria hyperborea*, *Ascophyllum nodosum* [46,47] and several bacteria strains (*Azotobacter*, *Pseudomonas*) [48]. This polysaccharide is present in the intercellular matrix, behaving like a gel containing sodium, calcium, magnesium, strontium and barium ions.

ALG is a salt of alginic acid that is structurally a block copolymer of 1→4 linked β-D-mannuronate (M) and α-L-guluronate (G) residues. The blocks of ALG are composed of homopolymeric regions of M and G residues that are known as M- and G-blocks, respectively, and heteropolymeric regions consisting of alternating M and G residues that are known as MG-blocks [49,50,51].

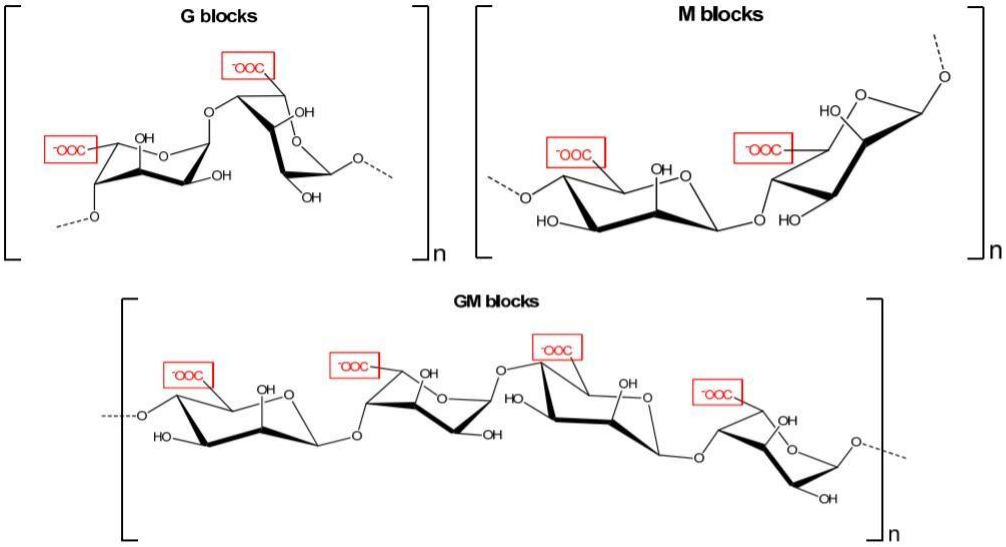

Figure 1.7. Structure of alginate. Image from reference [52].

Generally, ALG hydrogels are prepared from the precursor (an aqueous solution of ALG) by ionic cross-linking with divalent cations, such as Ca^{2+}, Sr^{2+}, or Ba^{2+}. Although the Ca^{2+} cation is not the most affinity with alginate, it is the most used because of its non-toxicity and low cost [53]. The water-soluble alginate is in its sodium salt form, where Na^{+} is ionically bound to alginate G blocks. In the presence of divalent cations, the gelation occurs when the G blocks interact with the divalent cations, thus replacing the Na^{+} associated with the carboxyl groups forming ionic bridges[49]. Therefore, the physical properties of the ALG hydrogels strongly depend on the M / G ratio, block sequence M

and G, G block length and molar mass[54]. The interaction between alginate molecules and calcium ions can be explained by the so-called "egg carton" model [55], where calcium ions fit between the alginate guluronic acid chains in a manner analogous to an egg within of an egg carton (figure 1.8).

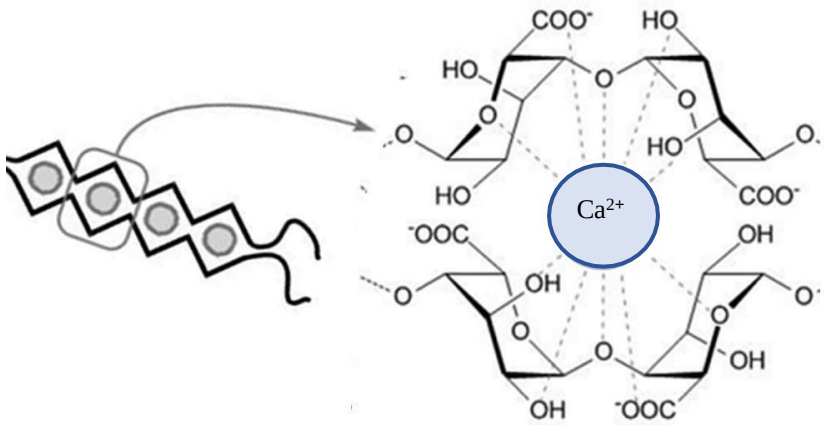

Figure 1.8. Interaction between divalent cation and alginate in the "egg-box model". Addaped from Destruel, P.-L., et al. [56].

Alginate is one of the hydrogel-based biomaterials that has more applications in the field of biomedical engineering due to its favourable properties, such as biocompatibility, biodegradability, non-antigenicity and its favourable ionic gelling ability that occurs at mild pH and temperature conditions, suitable for cells and for sensitive biomolecules such as proteins and nucleic acids [57]. Alginate hydrogels have application as skin dressings, controlled delivery of drugs and more recently in tissue engineering, since these gels have a structure very similar to the extracellular matrix [58].

To summarize, alginate has been extensively utilized in different tissues and organs such as skin [59], cartilage [60], bone tissue [61] and cardiac tissue [62] suggests their promising future for repair and regeneration applications. Alginate hydrogels are favourable for cell transplantation or immobilization and can be used to deliver cells to a desired site in vivo or provide a controlled 3D environment for new tissue formation in vitro[57].

1.4. Bioprinting applications

Bioprinting has been a rapidly growing field with a strong impact in the medical and pharmaceutical sciences, proving to be an extremely promising technology for the advancement of tissue manufacturing in relation to physiologically relevant tissue

constructs, tissue, organ and tissue models and organ-on-a-chip models. Numerous applications have been developed in life sciences, from the study of cellular mechanisms to the construction of tissues and organs for implantation, including, bone, skin, myocardial tissue, and blood vessels.

- **Bone**

Tissue engineering is one of the most hopeful approaches for developing engineered alternatives for damaged bones.

In 2013 Zhu, et al, studied adenovirus with human transforming growth factor-β1transfected bone marrow MSC combined with calcium alginate gel for tissue engineering purpose [63]. Luo et al., [64] studied 3D printing of alginate / gelatine scaffolds with homogeneous nano-apatite coating for bone tissue engineering. During the test the amount of phosphate in the printing inks was adjusted to control the thickness of the coating. Coated scaffolds had a higher Young's modulus than those lacking nanoapatite, a greater adsorption of proteins on the surface of the scaffolds, and a significant increase in the proliferation and osteogenic differentiation of rBMSCs. It being shown that these scaffolds will be great candidates for the engineering of bone tissue.

- **Cartilage**

Cartilage repair continues to be a major challenge, however recently 3D bioprinting strategies have been used to recreate this tissue.

Duong Nguyen and his team used pluripotent stem cells (iPSCs) from patients during surgery, and these cells were manipulated to revert to stem cells, which were then encapsulated in nanofibrillated cellulose material and printed using a 3D bioprinter. After a high survival of the cells, immediately after printing, the cells were subjected to a treatment with growth factors, which led to them to multiply and to differentiate correctly, thus forming cartilaginous tissue [65]. Yu et al. utilized a triaxial nozzle assembly to fabricate biocompatible cartilage-like tissues containing tubular channels. Cartilage progenitor cells were encapsulated in alginate, the main component of the bioink [66].

In the last year, Yang et al., used a hydrogel-based material to create synthetic meniscus for a plastic model of a knee. These hydrogels were printed at room temperature using a low-cost 3D printer, which did not prove to be a hindrance to the success of the work. This proved to be a huge advantage in regenerative medicine, since it proved to be an implant that combines strength with the elasticity of the original cartilage and the

biocompatibility of these materials supports the growth of the cells that allows the healing of the site in question [67].

- **Skin**

Artificial skin substitutes usually rely on biomaterials for skin restoration, while cell-cell therapies can help heal skin cells. New therapies range from novel naturally occurring extracellular matrix formulations to in situ delivery of stem cells.

In 2009, Lee et al. deposited keratinocytes and fibroblasts in a stratified arrangement using 3D bioprinting in vitro [68]. In this study, a robotic platform was used that prints the collagen precursor (type 1 of rat tail origin), following a layer of cells (fibroblasts and keratinocytes) intermittently. Printed cells retained their morphology and a highly viable proliferation of each cell layer was observed, thus demonstrating the ability to print and grow multi-layered hydrogel composites on a non-planar planar surface.

Michael et al. [69] showed successful 3D impression of a cell construct and subsequent tissue formation in full-thickness cutaneous wounds in vivo using a laser- assisted bioprinting (LaBP) technique where fibroblasts and keratinocytes were positioned on top of a stabilizing matrix (Matriderm®). Showing to be a promise to improve the quality of life of patients with burns.

Small scale 3D skin tissue models for cosmetics, drug and toxicity testing as well as tumour modelling are the most promising research avenues for clinical applicability in the short to mid-term before this technology can be translated to benefit reconstructive surgical patients.

- **Kidney**

An in-vitro model of the human proximal tubule interstitial interface can be fabricated by bioprinting of renal fibroblasts, endothelial cells and primary human renal proximal tubule epithelial cells [70]. The in vitro proximal tubule tissue can be used to study the mechanisms of nephrotoxicity and to investigate epithelial–interstitial interactions involved in kidney pathogenesis.

- **Cardiac tissue**

Cardiovascular disease is a major health problem worldwide, causing high morbidity and mortality and raising the cost of health care. The engineering of cardiac tissues has the potential to restore these damaged myocardial tissues [71].

In 2015, a research team led by Thomas Scheibel was able to mix spider silk with mouse fibroblast cells to generate gel using 3D printing. Silk molecules enveloped rat cells, providing a porous matrix for growth. The results show that spider silk is a great material for producing hydrogels and can be an effective base for restoring cardiac tissue [72].

- **Blood vessels**

Considering that there are tens of thousands of blood vessels in the human body, 3D printing has also been used in attempt to develop new viable alternatives for replacement if they fail. For example, recently a team from China was transplanted 3D-printed blood vessels made from stem cells into rhesus monkeys to promote vascularization, another method of creating blood vessels, was developed by Bertassoni et al., at Brigham and Women's Hospital, where they used a model of agarose fiber covered with hydrogel, able to build networks of microchannels that exhibited various architectural resources [73].

In 2007, Zhu, W., et al. [74] created a simple method to construct a network of blood vessels, this method consists of a continuous microscalemCOB printing platform, where cells mimic the composition of vascular cells encapsulated in hydrogels (GM- HA and GelMa). At the end of 2 weeks the results showed a complex tissue like the blood vessels, and that allowed the blood circulation. This strategy can be designed for example to create cardiac tissue that has complex networks of blood vessels, allowing to replace damaged heart muscle or for drug testing.

- **Organ-on-a-chip**

Organ-on-chips are microfluidic cell culture systems, are examples of physiological and natural substances that produce cells in the human body. These are coated with the viscera cells and their tiny fluidic channels which reproduce blood and / or airflow, as well as not human body. Its flexibility allows the chips to receive respiratory flows or muscle contractions. Another feature is its flexibility that allows its execution, behaviour and response at the cellular and molecular level [75].

One such example of an Organ-on-a-Chip is the Heart-on-a-chip which consists of a multi chamber array that replicates the tissue architecture in the heart. By modelling the electric impulses controlling the heart rate, Grosberg et al. were able to investigate the biological structure-to-function relationship [76].

Although an entire lung on a microfluidic chip has not yet been developed, Huh et al. Have succeeded in replicating the function of an alveolar-capillary membrane. To produce this membrane, collagen-coated polydimethylsiloxane (PDMS) was used for better cell adhesion, separating the epithelial cells in contact with the air on one side and the endothelial cells in contact with a fluid composed of nutrients instead of blood. The development of such solutions may become essential for the treatment of lung diseases [77].

These organs in chips show high potential for the future of medicine: the systematic use of organs in chips would help the pharmaceutical industry to save time and money, in addition to being possible to create a personalized treatment for each patient. In addition, it is possible to create tumours on chips, thus allowing the direct testing of tumours in the various treatments, since it is possible to reproduce the microenvironment in which cancer cells interact physically or chemically [78,79].

- **Drug delivery**

Currently the use of animal models has not been shown to be the most effective method in the pre-clinical trials, since it represents a time-consuming process with high maintenance costs, and the fact that there are differences between the physiology of these animal models and the human physiology, which can lead to a misinterpretation of results and consequently an incorrect prediction of human responses.

For that reasons drug delivery from three-dimensional (3D) structures is a rapidly growing research area, showing, in comparison with conventional methods, a process with high flexibility, good time savings and great production capacity [80]. Recently, the Food and Drug Administration approved even Levetiracetam tablets (SPRITAM®) [81]. This method continues to deserve special attention as it may result in disparate end-product qualities with improved controlled release, release of poorly water-soluble drugs, drug stability and facilitating drug-dose reduction without compromising efficacy, allowing thus creating medicines considering the pharmacogenetic profile of each patient [82].

- **Cancer models**

In 2017, the Ghent researchers combined cancer-associated fibroblasts (CAF) with tumor cell lines, thus finding that CAF increases both cancer cell survival and

angiogenesis, providing a privileged environment. The combination of these cells resulted in the formation of tumor structures (spheroids) in vitro, which demonstrated the importance of CAF in preclinical models [83].

One of the most aggressive forms of brain tumour is the high-grade glioma (GBM). Because of that Xingliang et al., are working to create a glioma stem cell model using 3D bioprinting, for this they created a porous gelatin/alginate / fibrinogen hydrogel structure that mimics the extracellular matrix of tumour stem cells. They made the hydrogel more stable by adding the cross-linker transglutima, a non-toxic transferase that naturally exists in the human body, to enhance gelatin. There were approximately 90% survival rates and high levels of cellular activity. This model provides a new alternative for the study of gliomagenesis, glioma stem cell biology, drug resistance and susceptibility to anticancer drugs in vitro [84].

The in vitro 3D models for ovarian cancer, is Dr. Bissel's main interest. In 1999 it was shown that normal breast epithelial cells cultured in Matrigel ™ form polarized acinar structures, which are morphologically similar to the terminal mammary lobes in vivo [85,86]. During the in vitro development of normal lobular acini, a single outer layer of cells in contact with the basal membrane expresses signs of preservation. The remaining cells in the centre of the lobe express stimulation signals and undergo apoptosis. This pattern of differential signalling contributes to the formation of properly developed acini with hollow lumens that resemble the normal lobular morphology of the breast. The evasion of these contextual cues causes the lumen to be filled with aberrantly proliferating epithelial cells, initiating signalling pathways that significantly alter cellular behaviour and potentially trigger early events in breast carcinogenesis.

2. References

1. Designation: F2792 − 12a. https://doi.org/10.1520/F2792-12A.

2. Apparatus for Production of Three-Dimensional Objects by Stereolithography. **1984**.

3. Wohlers, T.; Gornet, T. *History of Additive Manufacturing*; 2014.

4. Attaran, M. The Rise of 3-D Printing: The Advantages of Additive Manufacturing over Traditional Manufacturing. *Bus. Horiz.* **2017**, *60* (5), 677–688. https://doi.org/10.1016/j.bushor.2017.05.011.

5. Su, A.; Al'Aref, S. J. History of 3D Printing. In *3D Printing Applications in Cardiovascular Medicine*; Elsevier, 2018; pp 1–10. https://doi.org/10.1016/B978-0-12-803917-5.00001-8.

6. Mota, C.; Puppi, D.; Chiellini, F.; Chiellini, E. Additive Manufacturing Techniques for the Production of Tissue Engineering Constructs. *J. Tissue Eng. Regen. Med.* **2015**, *9* (3), 174–190. https://doi.org/10.1002/term.1635.

7. Herzog, D.; Seyda, V.; Wycisk, E.; Emmelmann, C. Additive Manufacturing of Metals. *Acta Mater.* **2016**, *117*, 371–392. https://doi.org/10.1016/J.ACTAMAT.2016.07.019.

8. Do, A.-V.; Khorsand, B.; Geary, S. M.; Salem, A. K. 3D Printing of Scaffolds for Tissue Regeneration Applications. *Adv. Healthc. Mater.* **2015**, *4* (12), 1742–1762. https://doi.org/10.1002/adhm.201500168.

9. Wong, K. V.; Hernandez, A. A Review of Additive Manufacturing. *ISRN Mech. Eng.* **2012**, *2012*, 1–10. https://doi.org/10.5402/2012/208760.

10. Molitch-Hou, M. Overview of Additive Manufacturing Process. In *Additive Manufacturing*; Elsevier, 2018; pp 1–38. https://doi.org/10.1016/B978-0-12-812155-9.00001-3.

11. Lee, J.-Y.; An, J.; Chua, C. K. Fundamentals and Applications of 3D Printing for Novel Materials. *Appl. Mater. Today* **2017**, *7*, 120–133. https://doi.org/10.1016/j.apmt.2017.02.004.

12. Panwar, A.; Tan, L. Current Status of Bioinks for Micro-Extrusion-Based 3D Bioprinting. *Molecules* **2016**, *21* (6), 685. https://doi.org/10.3390/molecules21060685.

13. Tofail, S. A. M.; Koumoulos, E. P.; Bandyopadhyay, A.; Bose, S.; O'Donoghue, L.; Charitidis, C. Additive Manufacturing: Scientific and Technological Challenges, Market Uptake and Opportunities. *Mater. Today* **2018**, *21* (1), 22–37. https://doi.org/10.1016/J.MATTOD.2017.07.001.

14. Ozbolat, I. T.; Yin Yu. Bioprinting Toward Organ Fabrication: Challenges and Future Trends. *IEEE Trans. Biomed. Eng.* **2013**, *60* (3), 691–699. https://doi.org/10.1109/TBME.2013.2243912.

15. Chang, R.; Nam, J.; Sun, W. Effects of Dispensing Pressure and Nozzle Diameter on Cell Survival from Solid Freeform Fabrication–Based Direct Cell Writing. *Tissue Eng. Part A* **2008**, *14* (1), 41–48. https://doi.org/10.1089/ten.a.2007.0004.

16. Melchels, F. P. W.; Domingos, M. A. N.; Klein, T. J.; Malda, J.; Bartolo, P. J.; Hutmacher, D. W. Additive Manufacturing of Tissues and Organs. *Prog. Polym. Sci.* **2012**, *37* (8), 1079–1104. https://doi.org/10.1016/j.progpolymsci.2011.11.007.

17. Wang, X.; Ao, Q.; Tian, X.; Fan, J.; Wei, Y.; Hou, W.; Tong, H.; Bai, S. 3D Bioprinting Technologies for Hard Tissue and Organ Engineering. *Mater. (Basel, Switzerland)* **2016**, *9* (10). https://doi.org/10.3390/ma9100802.

18. Pati, F.; Jang, J.; Lee, J. W.; Cho, D.-W. Extrusion Bioprinting. In *Essentials of 3D Biofabrication and Translation*; Elsevier, 2015; pp 123–152. https://doi.org/10.1016/B978-0-12-800972-7.00007-4.

19. Mao, A. S.; Mooney, D. J. Regenerative Medicine: Current Therapies and Future Directions. *Proc. Natl. Acad. Sci. U. S. A.* **2015**, *112* (47), 14452. https://doi.org/10.1073/PNAS.1508520112.

20. Langer, R.; Vacanti, J. P. Tissue Engineering.

21. Prendergast, M. E.; Solorzano, R. D.; Cabrera, D. Bioinks for Biofabrication: Current State and Future Perspectives. *J. 3D Print. Med.* **2017**, *1* (1), 49–62. https://doi.org/10.2217/3dp-2016-0002.

22. Hoffman, A. S. Hydrogels for Biomedical Applications. *Adv. Drug Deliv. Rev.* **2002**, *54* (1), 3–12. https://doi.org/10.1016/S0169-409X(01)00239-3.

23. Shoichet, M. S. Polymer Scaffolds for Biomaterials Applications. *Macromolecules* **2010**, *43* (2), 581–591. https://doi.org/10.1021/ma901530r.

24. Goldberg, M.; Langer, R.; Jia, X. Nanostructured Materials for Applications in Drug Delivery and Tissue Engineering. *J. Biomater. Sci. Polym. Ed.* **2007**, *18* (3), 241–268.

25. Hospodiuk, M.; Dey, M.; Sosnoski, D.; Ozbolat, I. T. The Bioink: A Comprehensive Review on Bioprintable Materials. *Biotechnol. Adv.* **2017**, *35* (2), 217–239. https://doi.org/10.1016/j.biotechadv.2016.12.006.

26. Kang, Y.; Jabbari, E.; Yang, Y. Integrating Top-Down and Bottom-Up Scaffolding Tissue Engineering Approach for Bone Regeneration. In *Micro and Nanotechnologies in Engineering Stem Cells and Tissues*; John Wiley & Sons, Inc.: Hoboken, New Jersey, 2013; pp 142–158. https://doi.org/10.1002/9781118574775.ch6.

27. Gopinathan, J.; Noh, I. Recent Trends in Bioinks for 3D Printing. *Biomater. Res.* **2018**, *22* (1), 11. https://doi.org/10.1186/s40824-018-0122-1.

28. Nolan, M. C.; Fuentes Caparró, A. M.; Dietrich, B.; Barrow, M.; Cross, E. R.; Bleuel, M.; King, S. M.; Adams, D. J. Optimising Low Molecular Weight Hydrogels for Automated 3D Printing †. *8426 | Soft Matter* **2017**, *13*, 8426. https://doi.org/10.1039/c7sm01694h.

29. Van Hoorick, J.; Declercq, H.; De Muynck, A.; Houben, A.; Van Hoorebeke, L.; Cornelissen, R.; Van Erps, J.; Thienpont, H.; Dubruel, P.; Van Vlierberghe, S. Indirect Additive Manufacturing as an Elegant Tool for the Production of Self-Supporting Low Density Gelatin Scaffolds. *J. Mater. Sci. Mater. Med.* **2015**, *26* (10), 247. https://doi.org/10.1007/s10856-015-5566-4.

30. Mahinroosta, M.; Jomeh Farsangi, Z.; Allahverdi, A.; Shakoori, Z. Hydrogels as Intelligent Materials: A Brief Review of Synthesis, Properties and Applications. *Mater. Today Chem.* **2018**, *8*, 42–55. https://doi.org/10.1016/J.MTCHEM.2018.02.004.

31. Kocen, R.; Gasik, M.; Gantar, A.; Novak, S. Viscoelastic Behaviour of Hydrogel-Based Composites for Tissue Engineering under Mechanical Load. *Biomed. Mater.* **2017**, *12* (2), 025004. https://doi.org/10.1088/1748-605X/aa5b00.

32. Pal, K.; Banthia, A. K.; Majumdar, D. K. *Polymeric Hydrogels: Characterization and Biomedical*

Applications-A Mini Review.

33. Hamidi, M.; Azadi, A.; Rafiei, P. Hydrogel Nanoparticles in Drug Delivery. *Adv. Drug Deliv. Rev.* **2008**, *60* (15), 1638–1649. https://doi.org/10.1016/j.addr.2008.08.002.

34. Diec, J.; Tilia, D.; Thomas, V. Comparison of Silicone Hydrogel and Hydrogel Daily Disposable Contact Lenses. *Eye Contact Lens Sci. Clin. Pract.* **2017**, 1. https://doi.org/10.1097/ICL.0000000000000363.

35. Koehler, J.; Brandl, F. P.; Goepferich, A. M. Hydrogel Wound Dressings for Bioactive Treatment of Acute and Chronic Wounds. *Eur. Polym. J.* **2018**, *100*, 1–11. https://doi.org/10.1016/J.EURPOLYMJ.2017.12.046.

36. Hennink, W. E.; van Nostrum, C. F. Novel Crosslinking Methods to Design Hydrogels. *Adv. Drug Deliv. Rev.* **2002**, *54* (1), 13–36.

37. Burdick, J. A.; Mauck, R. L.; Gerecht, S. Cell Stem Cell Forum To Serve and Protect: Hydrogels to Improve Stem Cell-Based Therapies Harsh Environments within Damaged and Diseased Tissues and Limited Retention and Survival of Injected Stem Cells Pose Major Challenges for Stem Cell Therapeutics Today. Here, We Discuss Promising Hydrogel-Based Strategies for Improving Engraftment and Viability of Transplanted Stem Cells and Stimulating Recruitment of Endogenous Stem Cells for Repair. *Stem Cell* **2016**, *18*, 13–15. https://doi.org/10.1016/j.stem.2015.12.004.

38. Pei, B.; Wang, W.; Fan, Y.; Wang, X.; Watari, F.; Li, X. Fiber-Reinforced Scaffolds in Soft Tissue Engineering. *Regen. Biomater.* **2017**, *4* (4), 257–268. https://doi.org/10.1093/rb/rbx021.

39. Ahmed, E. M. Hydrogel: Preparation, Characterization, and Applications: A Review. **2015**. https://doi.org/10.1016/j.jare.2013.07.006.

40. Ullah, F.; Othman, M. B. H.; Javed, F.; Ahmad, Z.; Akil, H. M. Classification, Processing and Application of Hydrogels: A Review. *Mater. Sci. Eng. C* **2015**, *57*, 414–433. https://doi.org/10.1016/j.msec.2015.07.053.

41. Chirani, N.; Yahia, H.; Gritsch, L.; Motta, F. L.; Chirani, S.; Faré, S. History and Applications of Hydrogels. *J. Biomed. Sci. 4* (2). https://doi.org/10.4172/2254-609X.100013.

42. Kumar, A. C.; Erothu, H. Synthetic Polymer Hydrogels. In *Biomedical Applications of Polymeric Materials and Composites*; Wiley-VCH Verlag GmbH & Co. KGaA: Weinheim, Germany, 2016; pp 141–162. https://doi.org/10.1002/9783527690916.ch6.

43. Kim, J. S.; Hong, S.; Hwang, C. Bio-Ink Materials for 3D Bio-Printing. *J. Int. Soc. Simul. Surg.* **2016**, *3* (2), 49–59. https://doi.org/10.18204/JISSiS.2016.3.2.049.

44. Hölzl, K.; Lin, S.; Tytgat, L.; Van Vlierberghe, S.; Gu, L.; Ovsianikov, A. Bioink Properties before, during and after 3D Bioprinting. *Biofabrication* **2016**, *8* (3), 032002. https://doi.org/10.1088/1758-5090/8/3/032002.

45. Khansari, M. M.; Sorokina, L. V.; Mukherjee, P.; Mukhtar, F.; Shirdar, M. R.; Shahidi, M.; Shokuhfar, T. Classification of Hydrogels Based on Their Source: A Review and Application in Stem Cell Regulation. *JOM* **2017**, *69* (8), 1340–1347. https://doi.org/10.1007/s11837-017-2412-9.

46. Smidsrød, O.; Skja˚k-Br1k, G. Alginate as Immobilization Matrix for Cells. *Trends Biotechnol.* **1990**, *8*, 71–78. https://doi.org/10.1016/0167-7799(90)90139-O.

47. Lee, K. Y.; Mooney, D. J. Alginate: Properties and Biomedical Applications. *Prog. Polym. Sci.* **2012**, *37* (1), 106–126. https://doi.org/10.1016/j.progpolymsci.2011.06.003.

48. Pawar, S. N.; Edgar, K. J. Alginate Derivatization: A Review of Chemistry, Properties and Applications. *Biomaterials* **2012**, *33* (11), 3279–3305. https://doi.org/10.1016/j.biomaterials.2012.01.007.

49. Sun, J.; Tan, H. Alginate-Based Biomaterials for Regenerative Medicine Applications. *Materials (Basel).* **2013**, *6* (4), 1285–1309. https://doi.org/10.3390/ma6041285.

50. Emami, Z.; Ehsani, M.; Zandi, M.; Foudazi, R. Controlling Alginate Oxidation Conditions for Making Alginate-Gelatin Hydrogels. *Carbohydr. Polym.* **2018**, *198*, 509–517. https://doi.org/10.1016/j.carbpol.2018.06.080.

51. Agüero, L.; Zaldivar-Silva, D.; Peña, L.; Dias, M. L. Alginate Microparticles as Oral Colon Drug Delivery Device: A Review. *Carbohydr. Polym.* **2017**, *168*, 32–43. https://doi.org/10.1016/J.CARBPOL.2017.03.033.

52. Vera, J.; Castro, J.; Gonzalez, A.; Moenne, A. Seaweed Polysaccharides and Derived Oligosaccharides Stimulate Defense Responses and Protection Against Pathogens in Plants. *Mar. Drugs* **2011**, *9* (12), 2514–2525. https://doi.org/10.3390/md9122514.

53. Ouwerx, C.; Velings, N.; Mestdagh, M. .; Axelos, M. A. . Physico-Chemical Properties and Rheology of Alginate Gel Beads Formed with Various Divalent Cations. *Polym. Gels Networks* **1998**, *6* (5), 393–408. https://doi.org/10.1016/S0966-7822(98)00035-5.

54. George, M.; Abraham, T. E. Polyionic Hydrocolloids for the Intestinal Delivery of Protein Drugs: Alginate and Chitosan — a Review. *J. Control. Release* **2006**, *114* (1), 1–14. https://doi.org/10.1016/j.jconrel.2006.04.017.

55. Grant, G. T.; Morris, E. R.; Rees, D. A.; Smith, P. J. C.; Thom, D. Biological Interactions between Polysaccharides and Divalent Cations: The Egg-Box Model. *FEBS Lett.* **1973**, *32* (1), 195–198. https://doi.org/10.1016/0014-5793(73)80770-7.

56. Destruel, P.-L.; Zeng, N.; Maury, M.; Mignet, N.; Boudy, V. In Vitro and in Vivo Evaluation of in Situ Gelling Systems for Sustained Topical Ophthalmic Delivery: State of the Art and Beyond. *Drug Discov. Today* **2017**, *22* (4), 638–651. https://doi.org/10.1016/j.drudis.2016.12.008.

57. Lee, K. Y.; Mooney, D. J. Alginate: Properties and Biomedical Applications. *Prog. Polym. Sci.* **2012**, *37* (1), 106–126. https://doi.org/10.1016/J.PROGPOLYMSCI.2011.06.003.

58. Szekalska, M.; Puciłowska, A.; Szymańska, E.; Ciosek, P.; Winnicka, K. Alginate: Current Use and Future Perspectives in Pharmaceutical and Biomedical Applications. *Int. J. Polym. Sci.* **2016**, *2016*, 1–17. https://doi.org/10.1155/2016/7697031.

59. Straccia, M.; d'Ayala, G.; Romano, I.; Oliva, A.; Laurienzo, P. Alginate Hydrogels Coated with Chitosan for Wound Dressing. *Mar. Drugs* **2015**, *13* (5), 2890–2908. https://doi.org/10.3390/md13052890.

60. Stein, S.; Strauss, E.; Bosco, J. Advances in the Surgical Management of Articular Cartilage Defects. *Cartilage* **2013**, *4* (1), 12–19. https://doi.org/10.1177/1947603512463226.

61. Zhao, L.; Weir, M. D.; Xu, H. H. K. An Injectable Calcium Phosphate-Alginate Hydrogel-Umbilical Cord Mesenchymal Stem Cell Paste for Bone Tissue Engineering. *Biomaterials* **2010**, *31* (25), 6502–6510. https://doi.org/10.1016/j.biomaterials.2010.05.017.

62. Dahlmann, J.; Krause, A.; Möller, L.; Kensah, G.; Möwes, M.; Diekmann, A.; Martin, U.; Kirschning, A.; Gruh, I.; Dräger, G. Fully Defined in Situ Cross-Linkable Alginate and Hyaluronic Acid Hydrogels for Myocardial Tissue Engineering. *Biomaterials* **2013**, *34* (4), 940–951. https://doi.org/10.1016/J.BIOMATERIALS.2012.10.008.

63. ZHU, S.; ZHANG, T.; SUN, C.; YU, A.; QI, B.; CHENG, H. Bone Marrow Mesenchymal Stem Cells Combined with Calcium Alginate Gel Modified by HTGF-B1 for the Construction of Tissue-Engineered Cartilage in Three-Dimensional Conditions. *Exp. Ther. Med.* **2013**, *5* (1), 95–101. https://doi.org/10.3892/etm.2012.765.

64. Luo, Y.; Li, Y.; Qin, X.; Wa, Q. 3D Printing of Concentrated Alginate/Gelatin Scaffolds with Homogeneous Nano Apatite Coating for Bone Tissue Engineering. *Mater. Des.* **2018**, *146*, 12–19. https://doi.org/10.1016/j.matdes.2018.03.002.

65. Nguyen, D.; Hägg, D. A.; Forsman, A.; Ekholm, J.; Nimkingratana, P.; Brantsing, C.; Kalogeropoulos, T.; Zaunz, S.; Concaro, S.; Brittberg, M.; et al. Cartilage Tissue Engineering by the 3D Bioprinting of IPS Cells in a Nanocellulose/Alginate Bioink. *Sci. Rep.* **2017**, *7* (1), 658. https://doi.org/10.1038/s41598-017-00690-y.

66. Yu, Y.; Zhang, Y.; Martin, J. A.; Ozbolat, I. T. Evaluation of Cell Viability and Functionality in Vessel-like Bioprintable Cell-Laden Tubular Channels. *J. Biomech. Eng.* **2013**, *135* (9), 091011. https://doi.org/10.1115/1.4024575.

67. Yang, F.; Tadepalli, V.; Wiley, B. J. 3D Printing of a Double Network Hydrogel with a Compression Strength and Elastic Modulus Greater than Those of Cartilage. *ACS Biomater. Sci. Eng.* **2017**, *3* (5), 863–869. https://doi.org/10.1021/acsbiomaterials.7b00094.

68. Lee, W.; Debasitis, J. C.; Lee, V. K.; Lee, J.-H.; Fischer, K.; Edminster, K.; Park, J.-K.; Yoo, S.-S. Multi-Layered Culture of Human Skin Fibroblasts and Keratinocytes through Three-Dimensional Freeform Fabrication. *Biomaterials* **2009**, *30* (8), 1587–1595. https://doi.org/10.1016/j.biomaterials.2008.12.009.

69. Michael, S.; Sorg, H.; Peck, C.-T.; Koch, L.; Deiwick, A.; Chichkov, B.; Vogt, P. M.; Reimers, K. Tissue Engineered Skin Substitutes Created by Laser-Assisted Bioprinting Form Skin-Like Structures in the Dorsal Skin Fold Chamber in Mice. *PLoS One* **2013**, *8* (3), e57741. https://doi.org/10.1371/journal.pone.0057741.

70. King, S. M.; Higgins, J. W.; Nino, C. R.; Smith, T. R.; Paffenroth, E. H.; Fairbairn, C. E.; Docuyanan, A.; Shah, V. D.; Chen, A. E.; Presnell, S. C.; et al. 3D Proximal Tubule Tissues Recapitulate Key Aspects of Renal Physiology to Enable Nephrotoxicity Testing. *Front. Physiol.* **2017**, *8*, 123. https://doi.org/10.3389/fphys.2017.00123.

71. Mosadegh, B.; Xiong, G.; Dunham, S.; Min, J. K. Current Progress in 3D Printing for Cardiovascular Tissue Engineering. *Biomed. Mater.* **2015**, *10* (3), 034002. https://doi.org/10.1088/1748-6041/10/3/034002.

72. Petzold, J.; Aigner, T. B.; Touska, F.; Zimmermann, K.; Scheibel, T.; Engel, F. B. Surface Features of Recombinant Spider Silk Protein EADF4(K16)-Made Materials Are Well-Suited for Cardiac Tissue Engineering. *Adv. Funct. Mater.* **2017**, *27* (36), 1701427. https://doi.org/10.1002/adfm.201701427.

73. Bertassoni, L. E.; Cecconi, M.; Manoharan, V.; Nikkhah, M.; Hjortnaes, J.; Cristino, A. L.; Barabaschi, G.; Demarchi, D.; Dokmeci, M. R.; Yang, Y.; et al. Hydrogel Bioprinted Microchannel Networks for Vascularization of Tissue Engineering Constructs. *Lab Chip* **2014**, *14* (13), 2202–2211. https://doi.org/10.1039/C4LC00030G.

74. Zhu, W.; Qu, X.; Zhu, J.; Ma, X.; Patel, S.; Liu, J.; Wang, P.; Lai, C. S. E.; Gou, M.; Xu, Y.; et al. Direct 3D Bioprinting of Prevascularized Tissue Constructs with Complex Microarchitecture. *Biomaterials* **2017**, *124*, 106–115. https://doi.org/10.1016/j.biomaterials.2017.01.042.

75. Bein, A.; Shin, W.; Jalili-Firoozinezhad, S.; Park, M. H.; Sontheimer-Phelps, A.; Tovaglieri, A.; Chalkiadaki, A.; Kim, H. J.; Ingber, D. E. Microfluidic Organ-on-a-Chip Models of Human Intestine. *Cell. Mol. Gastroenterol. Hepatol.* **2018**, *5* (4), 659–668. https://doi.org/10.1016/j.jcmgh.2017.12.010.

76. Grosberg, A.; Alford, P. W.; McCain, M. L.; Parker, K. K. Ensembles of Engineered Cardiac Tissues for Physiological and Pharmacological Study: Heart on a Chip. *Lab Chip* **2011**, *11* (24), 4165. https://doi.org/10.1039/c1lc20557a.

77. Khetani, S. R.; Bhatia, S. N. Microscale Culture of Human Liver Cells for Drug Development. *Nat. Biotechnol.* **2008**, *26* (1), 120–126. https://doi.org/10.1038/nbt1361.

78. SUN, W.; CHEN, Y.-Q.; LUO, G.-A.; ZHANG, M.; ZHANG, H.-Y.; WANG, Y.-R.; HU, P. Organs-on-Chips and Its Applications. *Chinese J. Anal. Chem.* **2016**, *44* (4), 533–541. https://doi.org/10.1016/S1872-2040(16)60920-9.

79. Esch, E. W.; Bahinski, A.; Huh, D. Organs-on-Chips at the Frontiers of Drug Discovery. *Nat. Rev. Drug Discov.* **2015**, *14* (4), 248–260. https://doi.org/10.1038/nrd4539.

80. Wang, C.-C.; Tejwani (Motwani), M. R.; Roach, W. J.; Kay, J. L.; Yoo, J.; Surprenant, H. L.; Monkhouse, D. C.; Pryor, T. J. Development of Near Zero-Order Release Dosage Forms Using Three-Dimensional Printing (3-DP^{TM}) Technology. *Drug Dev. Ind. Pharm.* **2006**, *32* (3), 367–376. https://doi.org/10.1080/03639040500519300.

81. FDA Approves The First 3D Printed Drug Product - The Business Journals https://www.bizjournals.com/prnewswire/press_releases/2015/08/03/MM64802 (accessed Jun 10, 2018).

82. Khaled, S. A.; Burley, J. C.; Alexander, M. R.; Yang, J.; Roberts, C. J. 3D Printing of Tablets Containing Multiple Drugs with Defined Release Profiles. *Int. J. Pharm.* **2015**, *494* (2), 643–650. https://doi.org/10.1016/j.ijpharm.2015.07.067.

83. De Jaeghere, E.; De Vlieghere, E.; Van Hoorick, J.; Van Vlierberghe, S.; Wagemans, G.; Pieters, L.; Melsens, E.; Praet, M.; Van Dorpe, J.; Boone, M. N.; et al. Heterocellular 3D Scaffolds as Biomimetic to Recapitulate the Tumor Microenvironment of Peritoneal Metastases in Vitro and in Vivo. *Biomaterials* **2018**, *158*, 95–105. https://doi.org/10.1016/j.biomaterials.2017.12.017.

84. Dai, X.; Ma, C.; Lan, Q.; Xu, T. 3D Bioprinted Glioma Stem Cells for Brain Tumor Model and Applications of Drug Susceptibility. *Biofabrication* **2016**, *8* (4), 045005. https://doi.org/10.1088/1758-5090/8/4/045005.

85. Petersen, O. W.; Rønnov-Jessen, L.; Howlett, A. R.; Bissell, M. J. Interaction with Basement Membrane Serves to Rapidly Distinguish Growth and Differentiation Pattern of Normal and Malignant Human Breast Epithelial Cells. *Proc. Natl. Acad. Sci. U. S. A.* **1992**, *89* (19), 9064–9068.

86. Bissell, M. J.; Weaver, V. M.; Leli~vre, S. A.; Wang, F.; Petersen, O. W.; Schmeichel, K. L. Tissue Structure, Nuclear Organization, and Gene Expression in Normal and Malignant Breast I. *CANCER Res.* **1999**, *59*, 1757–1764.

Chapter II

3D Printing of soft hydrogel structures in a support bath

3D Printing of soft hydrogel structures in a support bath

Sousa, L.[1], Oliveira, J.M. [2] and Mano, J.F.[1#]

[1]Department of Chemistry, CICECO – Aveiro Institute of Materials, University of Aveiro, Campus Universitário de Santiago, 3810-193, Aveiro, Portugal

[2] Escola Superior Aveiro Norte, University of Aveiro,
Parque do Cercal, 3720-509 Santiago de Riba-Ul, Oliveira de Azeméis, Portugal

[#]Corresponding author:
João F. Mano
E-mail: jmano@ua.pt

Abstract

In tissue engineering, 3D bioprinting technologies with hydrogels are potentially capable of making tissues and organs or replacing damaged or even missing tissues.

Hydrogels have been extensively investigated and applied in regenerative medicine because of their similarity to the extracellular matrix, providing a highly hydrated environment for cell proliferation. However, their application in bioprinting technologies is still scarce, since the hydrogels are soft materials with low viscosity, presenting little structural resistance when printed in air.

In the recent years, some attempts on the development of complex hydrogel structures have been performed. Here, we analyze the existing liquid or granular medium to support complex printing of hydrogel structures to be apply in tissue engineering and regenerative medicine. This review also summarizes the challenges and provides new perspectives for future directions in this field.

Keywords: support bath, granular medium, freeform hydrogels, complex soft structures.

1. Introduction

The use of soft materials, including elastomers and hydrogels, is a promising approach to regenerative medicine.

Hydrogels are one of the most widely used materials classes in tissue engineering, due to their outstanding properties, such as good biocompatibility and good permeability. However, because of their low stiffness[1,2] hydrogel printed structures can easily collapse in air, losing their shape. Thus, the use of these materials to construct complex 3D structures without any support structure is a huge challenge [3].

When we talk about this type of materials for 3D printing, many parameters can affect the final product. The speed with which the 3D printer's head moves, the consistency of the gel bath in which the product is printed, and the concentration of the "ink" material are just a few of the variables that can affect the final product. On each printout, there may be dozens of parameters to consider and far more possible combinations of them.

Once the design challenge is over, it is expected that these soft materials can be used to create living constructs. However, such constructs have high fracture strength, as they need to withstand high internal and external mechanical loads and must be capable of transporting fluids, in order to allow the exchange of oxygen and metabolites [4,5]. Hence new limitations arise, since these physical and metabolic needs require that the fabricated structures have a dense vasculature capable of withstanding high loads, and that this is puncturable of way to allow these exchanges. Thus, mimicking an organ or tissue that meets all these characteristics is a process with high complexity.

All these barriers have recently attracted some researchers to investigate this area, beginning to try to print complex 3D structures with high resistance in a liquid medium, which will be the main topic approached in this review.

2. Bioprinting in liquid medium

Hydrogels are three-dimensional (3D) polymer networks composed of chains of cross-linked hydrophilic polymers that can absorb and retain large amounts of water [6]. Hydrogels are attractive as scaffolding material, since their porous structure ensures nutrient supply and removal of metabolites, which is essential for assuring cellular

functions [7]. However, as already discussed above, designing a hydrogel-based structure that does not collapse is a major challenge.

In 2017, You, F.,[8] used a bioprinting technique to fabricate hydrogel scaffolds with well-defined internal structure and interconnected porosity for tissue engineering applications, using a thermal crosslinking process and submerged ion crosslinking processes.

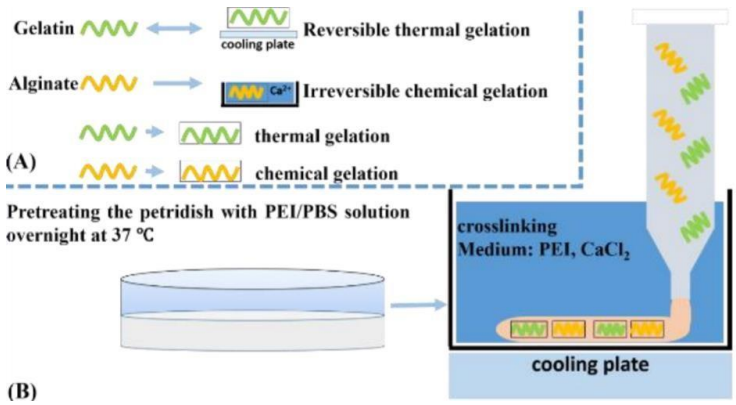

Figura 2.1. (A) Underlying mechanism; (B) Schematics of the hydrogel gelation mechanism based on reversible thermal gelation of gelatin and irreversible chemical gelation of alginate [8].

As base material was used gelatin and a natural polysaccharide, sodium alginate, which in the presence of calcium ions crosslinks ionically thus forming a gel [9]. This composite hydrogel precursor was printed on the cross-linking medium containing calcium chloride and Polyethylenimine (PEI) with low molecular weight which has shown great potential for use in the field of tissue engineering and regenerative medicine [10].

To manufacture hydrogel scaffolds, the liquid hydrogel precursor is charged to the dispensing head, dispensed by pressurized air at 37°C and cross-linked immediately after dispensing. This instantaneous action is brought about by the presence of gelatin which induces the immediate gelation of the preheated hydrogel precursors upon contact with the cooled substrate due to the gel thermoreversibility and the presence of calcium ions. The combination of these two cross-linking processes helps maintain the geometry of the wires dispensed, facilitating long-term stability.

Therefore, this technique was used to produce porous hydrogel scaffolds in order to solve the problems. The scaffold geometries, including the orientation of the layers and the spacing between them, were adjusted for bioprinting and their influence on the mechanical properties of the scaffold was investigated. The results showed that there was

significant influence of the internal design on the mechanical performance of the printed hydrogel scaffolds and the porosity, the area of contact between the filaments and the spacing variation were three key factors that influence the mechanical performance of the scaffolds.

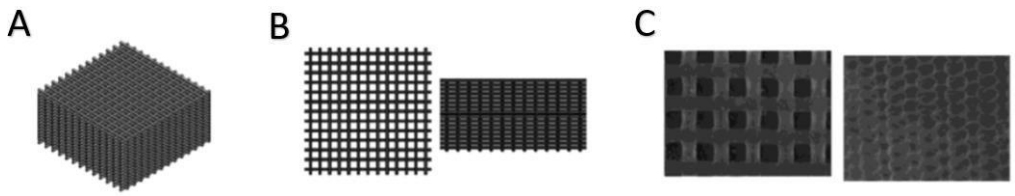

Figura 2.2. (A) CAD 3D model; (B) CAD 2D sections (top view and cross section); (C) Microscopic images (top view and cross section). Addapted from reference [8].

This biofabrication technique and the porous hydrogel supports obtained may support high cell viability and deposition of cartilaginous ECM. The technique may also be compatible with various soluble biomaterials because of their hydrophilic nature. As such, this biofabrication technique is a versatile platform with potential applications for tissue cartilage engineering.

3. Bioprinting in granular medium

3.1. Carbopol

In 2016, Bhattacharjee et al., [11] developed a granular medium, made up of Carbopol microgels, capable of supporting complex three-dimensional structures. Carbopol is made of carbomer polymers interconnected with each other, forming a microgel structure, which allows movement to be performed [12]. The use of Carbopol gels has some advantages among which the fact that they are anionic hydrogels with good buffering capacity that contributes to the maintenance of the desired pH, offers high viscosity even at low concentrations, has bioadhesive properties and good thermal stability [13]. However, in this case the carbopol is not an ideal material for the construction of these gels, since they quickly reach the properties of the stable material after abrupt changes in applied shear stress.

In order to explore the stability and precision of the impression in granular gels, a series of complex structures were produced. One of them is a DNA model of 4 cm in length, made of fluorescent polystyrene microspheres. These polymer and colloid based

structures such as (PVA) were printed on aqueous granular gel and polydimethylsiloxane (PDMS) on an oil-based granular gel. After printing the structures were visualized with confocal fluorescence microscopy, revealing that the structures had an excellent stability in the medium, and no change in the characteristics of the initial form was visible. In view of these results we can affirm that printing on granular gel medium provides precision and stability [11].

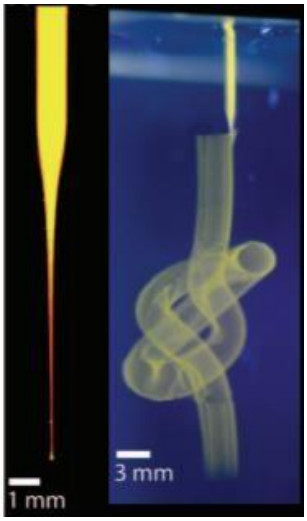

Figura 2.3. (A) Injection tip filled with fluorescent microsphere suspension, photographed under UV illumination. (B) Continuous node imprinted with aqueous suspension of fluorescent microspheres in aqueous granular gel [11].

Despite these evidences, the creation of hydrogel structures with high detail still remains a challenge. Several complex multi-scale structures were then printed on the granular gel medium made of crosslinked PVA hydrogels and fluorescent colloids. One of the models drawn was an octopus, made with eight helical shells mimicking the tentacles and a bulbous shell like the body. The structure remained stable throughout the printing process until the end of ultraviolet crosslinking, which begins immediately after the end of writing and lasts for about 6 hours. Subsequently the powder was immersed in a gently swirling water bath, in order to facilitate the removal process. It was then verified that the octopus maintained its structural integrity, even without support bath [11].

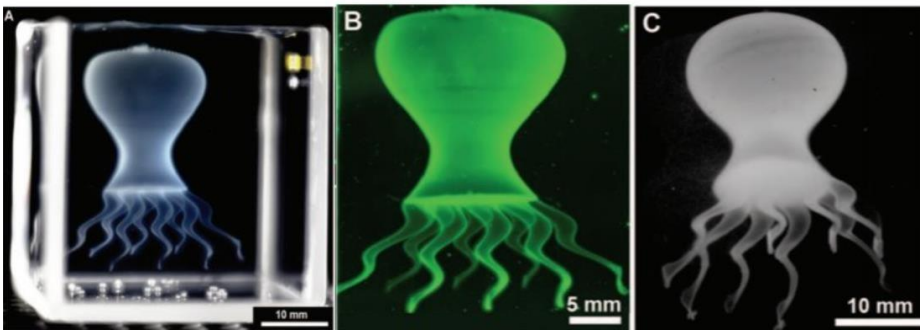

Figura 2.4. (A) Model of an octopus made from various parts of hydrogel connected to a stable and complex surface prior to polymerization. (B) Fluorescence image of the model after polymerization, retained in granular gel. (C) The polymerized octopus's model after removal of the granular gel, floating in the water [11].

Bioengineering has as main objective to create living tissues capable of transporting fluids, for exchange of oxygen and metabolites. However, these metabolic needs require the manufacture of macroscopic structures with a dense vasculature and larger cell aggregates [14]. For this purpose, a complex tubular network made of a biocompatible PVA formulation was fabricated, composed of conical tubes connected by quaternary crosses that transform smoothly, with convex and concave curves. Achieving a continuous and robust structure. When placed in a water bath, it is possible to visualize the flow of its branches.

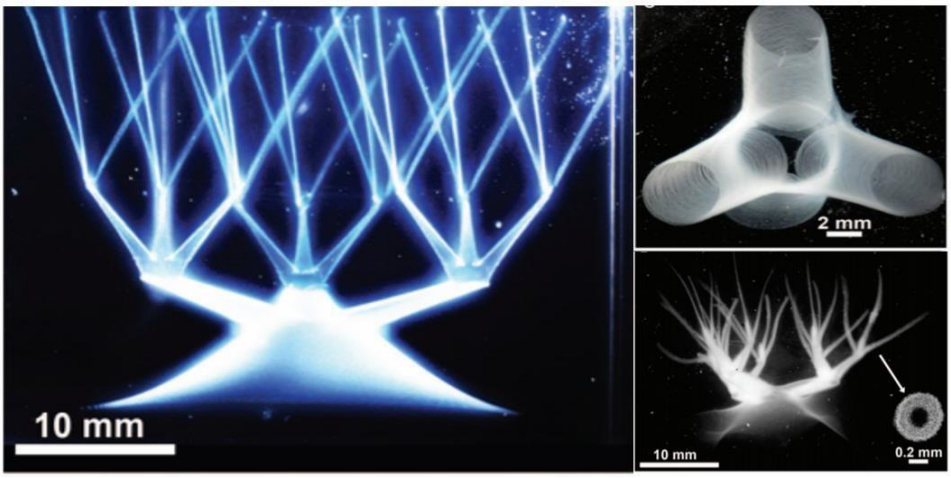

Figura 2.5. (A) Continuous network of hollow vessels. (B) Truncated vases around a junction. (C) Reticulated network, removed from the granular gel, photographed freely floating in water [11].

In this context, living tissue cells were cultured in a granular gel culture medium, prepared using cell growth medium as the solvent. Migration and cell division were observed, which demonstrated the potential of the granular gel as a suitable medium for

3D cell culture. Vascular networks were printed from human aortic endothelial cells (HAECs), without the PVA matrix, where using fluorescence confocal microscopy it was possible to visualize the hollow tube with walls made of HAECs. Using a very similar procedure, a Madin-Darby canine kidney (MDCK) was developed. MCF10A epithelial cell lines were also printed at variable speeds, giving equal thicknesses, which represents an extremely positive point, since epithelial and endothelial tissues throughout the body are composed of layers with only one cell of thickness.

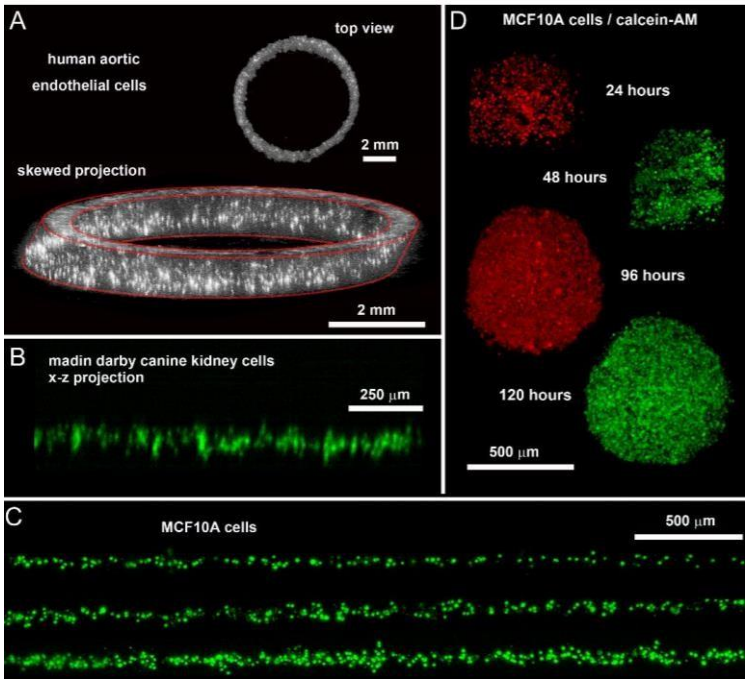

Figura 2.6. (A) A structure written only of living cells, attached to granular gel growth media, visualized with confocal fluorescence microscopy. (B) Madin Darby cells canine renal cells printed on the granular gel medium. (C) Long straight lines of MCF10A epithelial cells printed at different speeds. (D) Cell viability of MCF10A cells in the granular gel medium. The cells were incubated and monitored over five days, all cells stained with calcein-AM and photographed one hour after dyeing. The time points of 24 and 48 hours correspond to the same spheroid, where red calcein was used on the first day, and calcein green was used on the second day. Red and green calcein were used for a different spheroid on the fourth day and five, respectively [11].

There are still several limits to be defined, such as size, speed, precision and materials for structures printed on granular gels, but this medium has many advantages for the creation of complex multidimensional structures, which may translate into being immediately integrated into several areas, from tissue and organ engineering to flexible electronics.

The development of the manufacture of free-form flexible structures has been stimulated by several advances in materials and manufacturing technologies. Due to its properties, such as mechanical stiffness, swelling, degradation, cell binding and binding or release of bioactive molecules, alginate is one of the most widely used materials in tissue engineering [15].

Another problem raised using soft materials is that gelling is done during printing, which causes the nozzle to clog due to the surface tension created by the proximity of the nozzle to the crosslinking solution bath. To counter the drawbacks of this technique *Jin, Y. et al.*, [16] developed a novel approach based on gelation in 2 steps, based on reversible thermal gelation of gelatin and ionic gelation of sodium alginate. In this work, it was used as support bath Carbopol micro gels support granular, which as previously mentioned transits between the fluid and solid states, showing to be an ideal support material for the alginate extrusion, since it allows the filaments to be extruded freely in the bath, solidifying rapidly, allowing stability layer by layer until the structure is complete. The bioink, consisting of sodium alginate (NaAlg) and gelatin, is extruded to make a branched structure layer by layer in the Carbopol granular gel bath at room temperature.

Once the gelatin is gelatinised, the printed structure is removed and placed in a sodium chloride (NaCl) bath to swell and collapse the residual granular microgels of Carbopol. Finally, the clean structure without Carbopol is immersed in an ionic crosslinking solution at 37 ° C for 24 hours, obtaining tubular structures based on alginate [16].

After the printed structure, a DMEM solution supplemented with red dye flows through the alginate / gelatin structure, allowing to show that the Carbopol has all been cleared from the lumen and further showing that the structure is perfusable.

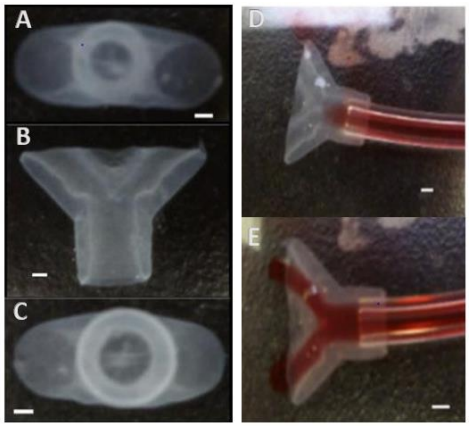

Figura 2.7. Alginate structure printing. (A, B e C) Different views of an alginate structure imprinted on a Carbopol bath (D e E) Lumen test after removal of Carbopol using a stained solution. Addapted from reference [16].

This new approach was applied for the printing of tubular constructs using bioink based on NIH 3T3 murine fibroblasts containing alginate and gelatin. Since alginate structures made using this technique have better mechanical properties than those made using the "gelling during printing" approach.

There are numerous technological advances being made in the biomaterial component of 3D printing, whether with new materials and compounds to be printed or in new printing processes that are expanding the print resolution or our ability to control the structure of the material.

The polydimethylsiloxane elastomer (PDMS) due to its characteristics is used in a wide range of applications, however it is not a good choice when we speak of 3D printing of complex structures, since it is a very little elastic material, thus requiring a support during printing [17]. Hinton et al., [18] reported this obstacle to the use of PDMS, and based on results from other work shown earlier, it was hypothesized that a hydrophilic microparticulate carrier bath could support the embossed impression of the PDMS.

Thus, this group developed a new printing method, Reversible Forging Reversible (FRE), designed to freely print complex structures, using Carbopol as support. Due to the combination of the immiscibility of the hydrophobic PDMS in the hydrophilic Carbopol, the extruded PDMS prepolymer could maintain a stable form within the carrier for curing times up to 72 h. After printing and curing, Carbopol was removed using phosphate buffered saline to reduce Carbopol yield stress, leaving only the PDMS structure [18].

In order to prove the applicability of this method, the Sylgard 184 PDMS was used to print linear and helical filaments through continuous extrusion and cylindrical and helical tubes through layer-by-layer fabrication. These tests have determined that hydrophobic polymers with low viscosity and long curing times can be printed in 3D using a hydrophilic carrier.

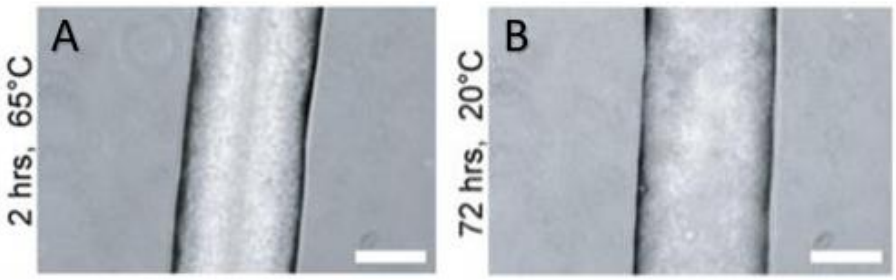

Figura 2.8. PDMS prepolymer filaments extruder and cured at different temperatures and in different Carbopols are dimensionally stable. (A e B) PDMS filaments extruded into Carbopol 940 and cured at 65 °C for 2 h and 20 °C for 72 h, respectively [18].

As proof of concept of this technology were printed a series of PDMS structures, focusing on tubular fluidic networks. The results demonstrate wide versatility of the FRE printing approach for the manufacture of 3D PDMS.

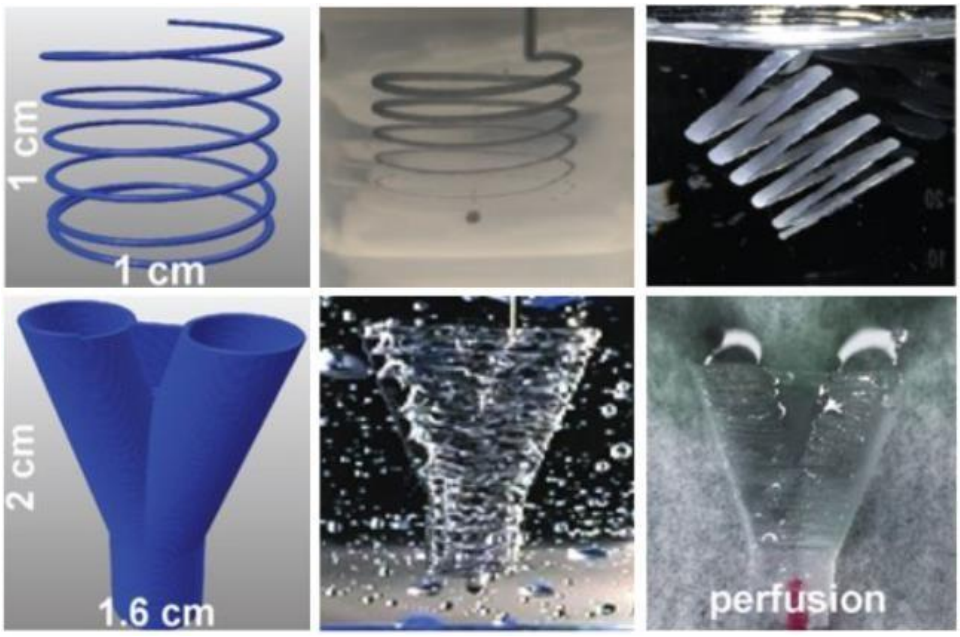

Figura 2.9. PDMS structures printed using the FRE technique on Carbopol support. (A) G-code for helical structure. (B) Carbopol gel can support freeform extrusion. (C) Extruded form in the Carbopol identical to the G code. (D) G-code of tubular structure. (E) The FRE printed PDMS bifurcation embedded in Carbopol. (F) Perfusion of dye through the bifurcation, splitting fluid flow [18].

This methodology may be applicable to a wide range of materials, and the fact that this printing platform is open source will accelerate research, enabling easy adoption of the technology using affordable and widely available 3D printers.

3.2. Gelatin microparticles

Several groups also attempted to overcome the problem of printing with soft materials, including Hinton et al., [19] which made the freely reversible incorporation of suspended hydrogels, also known as the FRESH method, which allows the bioimpression of soft materials such as collagen or alginate.

The method uses a hydrogel bath as a temporary and thermo-reversible support of fragile materials. To create this bath, the gelatin was mixed in $CaCl_2$ in a solution and gelled for 12 hours at 4 ° C, to which further $CaCl_2$ was added at 4 ° C and the contents thereof were mixed for a period of 30 to 120 s in a mixer of consumption grade. Thereafter, the mixed gelatin suspension was charged into conical tubes and centrifuged

at 4200 rpm for 2 min, causing the suspension particles to settle out of the suspension. The supernatant was removed and replaced with $CaCl_2$. The suspension was again stirred in suspension and centrifuged again. This process was repeated until no bubbles were observed on the top of the supernatant, which indicated that most of the soluble gelatin was removed.

This gelatin microparticle hydrogel features a plastic rheology of Bingham [20], which allows the printing needle to flow freely while the soft biomaterials are extruded. After the impression of the scaffolding is completed, the dish is heated to 37 degrees Celsius, liquefying the gelatin bath in order to release the printed structure.

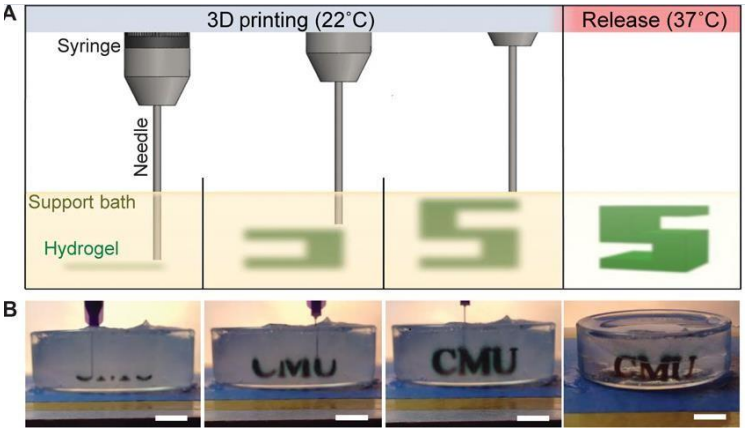

Figura 2.10. Freeform reversible embedding of suspended hydrogels technique. (A) A scheme of the FRESH process showing the hydrogel (green), such as collagen or alginate, being extruded and crosslinked into the gelatin mud support bath. The 3D object is built layer by layer and, when complete, is released by heating at 37 ° C and melting the gelatin. (B) Images of the letters "CMU" FRESH printed in alginate (black) [19].

One application of this technique is the use of magnetic resonance imaging (MRI) to print patient-specific scaffolds for designing tissues. Thus, through magnetic images a coronary arterial tree was made, made of materials such as fibrin, hyaluronic acid and alginate, with solid walls and an open lumen. Since we have already mentioned characteristics such as wall thickness, the diameter of the lumen and the density can be adapted according to the anatomy of each patient. The coronary arteries supply blood to the heart, which makes it important for the drawn arterial tree to be perforated, which has occurred, and this technique is a major advance for myocardial revascularization surgeries.

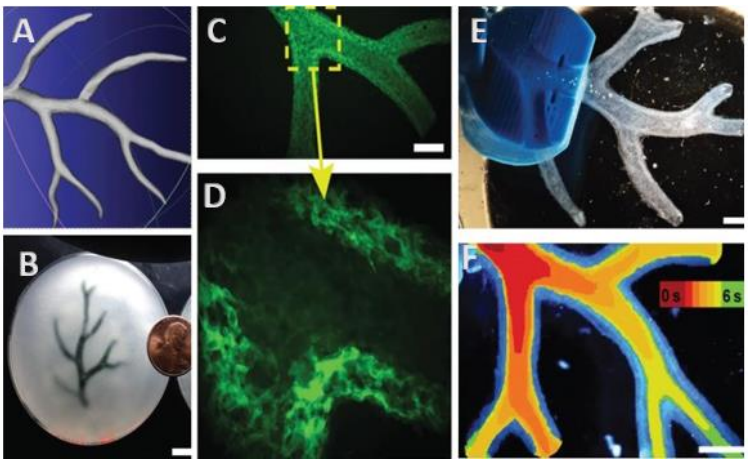

Figura 2.11. (A) Model of a section of a human coronary arterial tree. (B) Arterial tree printed in alginate (black) and soaked in the gelatin carrier bath. (C) A section of the arterial tree printed in fluorescent alginate (green) and photographed in 3D to show the hollow lumen and multiple bifurcations. (D) Enlarged view of the arterial tree shows vessel wall and well-formed lumen. (E) A dark field image of the arterial tree mounted in an infusion set to position a syringe at the root of the tree. (F) An image with a time lapse of 0 to 6 s to show the flow through the lumen [19].

This technique creates a more complex architecture, like an embryonic heart. The 3D model of the embryonic chick heart was generated from 3D optical data from a fluorescently labeled heart, from these images it is possible to identify the macrostructure and microstructure of the ECM, thus allowing the organ impression with extreme precision.

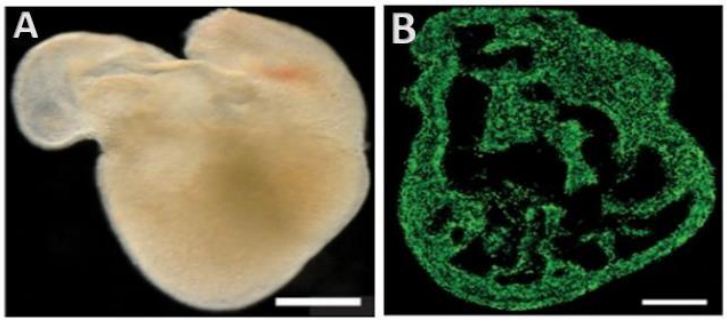

Figure 2.12. FRESH printed scaffolds with complex internal and external architectures. (A) A dark field image of an explanted embryonic chick heart. (B) A cross section of the heart printed in 3D in fluorescent alginate (green) showing the re-creation of the internal trabecular structure from the CAD model [19].

The results of this work show the ability to fabricate several complex 3D biological structures from natural soft biopolymers such as alginate, fibrin and type I collagen, which are crosslinked by ionic, enzymatic and pH / thermally mechanical processes, respectively. The low cost of FRESH and the ability to print a range of hydrogels in 3D should allow the expansion of bioprinting in several areas, such as tissue engineering.

4. Final Remarks

The development of new and effective methods for 3D printing of soft materials to create complex structures represents a tremendous advance for tissue engineering. Since we have seen that it is possible to use soft materials, such as alginate or fibrin, to create complex structures capable of mimicking tissues and organs, making it more convenient to replace or repair damaged or missing tissues or organs.

Hydrogel scaffolds with well-defined porous structures are important for tissue engineering. The 3D bioplotting technique combined with the thermal / submerged ionic crosslinking process in a PEI and calcium chloride bath was used to fabricate hydrogel alginate structures. However, this technique is only functional with respect to standard structures, since the PEI does not have rheological properties, so it does not allow to print complex structures without collapsing.

The search for sustainable support media capable of supporting complex structures led Hinton, J., et al., to develop a granular medium based on gelatin microparticles, which proved to be very promising, since it was possible to create complex structures, such as arterial tree with perfusion capacity. However, the production of the gelatin microparticles is a time-consuming process: mixing a solid block of gelatin to break down the hydrogel into microparticles; requires multiple centrifugations to recover the microparticles.

The potential of granular media based on Carbopol has also been investigated. Previous studies have shown that there is unquestionable potential in the application of Carbopol in tissue engineering, however it has some toxicity, and in addition the Carbopol polymerization process requires a long UV curing time.

Further research must be carried out in order to obtain a support bath that has the ideal characteristics (including good biocompatibility and easy processing for a scalable printing process) for the construction of complex structures capable of replacing missing or damaged tissues.

5. Aims

The global aim of this thesis is the development of a new methodology to design freeform alginate hydrogels by 3D printing in a biocompatible and scalable liquid medium, which enable to maintain the structural integrity of the hydrogel structure. This liquid support bath will be based on viscous solutions of xanthan gum derivatives, which is an extracellular polysaccharide with attractive rheological and biological properties. Furthermore, according to the chemical versatility of the xanthan gum, it is also envisioned the fabrication of a XG derivative with photocrosslinkable moieties where it should be possible to print microchannels alginate hydrogels following by the chemical crosslinking of the liquid medium as a support hydrogel. Such alginate-based microchannels will work as fugitive ink hydrogels allowing the formation of perfusable engineered constructs for advanced biomedical applications.

Briefly, the specific goals are:

- Deposition and ionic crosslinking of alginate hydrogels in xanthan gum liquid bath;
- Production and removal of complex hydrogel structures without deformation or collapse;
- Evaluation of the biocompatibility support bath and ability to keep cell alive during printing process;
- Fabrication of a perfusable device through 3D-printing of alginate hydrogel as fugitive ink within a photocrosslinked xanthan gum based hydrogel;
- Evaluation of the perfusion extension.

6. References

1. Hassan, P. A.; Verma, G.; Ganguly, R. Soft Materials — Properties and Applications. In *Functional Materials*; Elsevier, 2012; pp 1–59. https://doi.org/10.1016/B978-0-12-385142-0.00001-5.
2. MUROI, H.; HIDEMA, R.; GONG, J.; FURUKAWA, H. Development of Optical 3D Gel Printer for Fabricating Free-Form Soft ^|^amp; Wet Industrial Materials and Evaluation of Printed Double-Network Gels. *J. Solid Mech. Mater. Eng.* **2013**, *7* (2), 163–168. https://doi.org/10.1299/jmmp.7.163.
3. Kim, D. S. (Danny); Kao, Y.-T.; Tai, B. L. Hydrostatic 3D-Printing for Soft Material Structures Using Low One-Photon Polymerization. *Manuf. Lett.* **2016**, *10*, 6–9.

https://doi.org/10.1016/j.mfglet.2016.08.002.

4. Taylor, D.; O'Mara, N.; Ryan, E.; Takaza, M.; Simms, C. The Fracture Toughness of Soft Tissues. *J. Mech. Behav. Biomed. Mater.* **2012**, *6*, 139–147. https://doi.org/10.1016/j.jmbbm.2011.09.018.
5. Paulsen, S. J.; Miller, J. S. Tissue Vascularization through 3D Printing: Will Technology Bring Us Flow? *Dev. Dyn.* **2015**, *244* (5), 629–640. https://doi.org/10.1002/dvdy.24254.
6. Kopecek, J. Hydrogel Biomaterials: A Smart Future? *Biomaterials* **2007**, *28* (34), 5185–5192. https://doi.org/10.1016/j.biomaterials.2007.07.044.
7. You, F.; Wu, X.; Zhu, N.; Lei, M.; Eames, B. F.; Chen, X. 3D Printing of Porous Cell-Laden Hydrogel Constructs for Potential Applications in Cartilage Tissue Engineering. *ACS Biomater. Sci. Eng.* **2016**, *2* (7), 1200–1210. https://doi.org/10.1021/acsbiomaterials.6b00258.
8. You, F.; Wu, X.; Chen, X. 3D Printing of Porous Alginate/Gelatin Hydrogel Scaffolds and Their Mechanical Property Characterization. *Int. J. Polym. Mater. Polym. Biomater.* **2017**, *66* (6), 299–306. https://doi.org/10.1080/00914037.2016.1201830.
9. Kirchmajer, D. M.; Gorkin III, R.; in het Panhuis, M. An Overview of the Suitability of Hydrogel-Forming Polymers for Extrusion-Based 3D-Printing. *J. Mater. Chem. B* **2015**, *3* (20), 4105–4117. https://doi.org/10.1039/C5TB00393H.
10. Li, L.; He, Z.-Y.; Wei, X.-W.; Wei, Y.-Q. Recent Advances of Biomaterials in Biotherapy. *Regen. Biomater.* **2016**, *3* (2), 99–105. https://doi.org/10.1093/rb/rbw007.
11. Bhattacharjee, T.; Zehnder, S. M.; Rowe, K. G.; Jain, S.; Nixon, R. M.; Sawyer, W. G.; Angelini, T. E. Writing in the Granular Gel Medium. *Sci. Adv.* **2015**, *1* (8), e1500655–e1500655. https://doi.org/10.1126/sciadv.1500655.
12. Islam, M. T.; Rodríguez-Hornedo, N.; Ciotti, S.; Ackermann, C. Rheological Characterization of Topical Carbomer Gels Neutralized to Different PH. *Pharm. Res.* **2004**, *21* (7), 1192–1199.
13. Barry, B. W.; Meyer, M. C. The Rheological Properties of Carbopol Gels I. Continuous Shear and Creep Properties of Carbopol Gels. *Int. J. Pharm.* **1979**, *2* (1), 1–25. https://doi.org/10.1016/0378-5173(79)90025-5.
14. Chan, B. P.; Leong, K. W. Scaffolding in Tissue Engineering: General Approaches and Tissue-Specific Considerations. *Eur. Spine J.* **2008**, *17* (S4), 467–479. https://doi.org/10.1007/s00586-008-0745-3.
15. Lee, K. Y.; Mooney, D. J. Alginate: Properties and Biomedical Applications. *Prog. Polym. Sci.* **2012**, *37* (1), 106–126. https://doi.org/10.1016/j.progpolymsci.2011.06.003.
16. Jin, Y.; Compaan, A.; Bhattacharjee, T.; Huang, Y. Granular Gel Support-Enabled Extrusion of Three-Dimensional Alginate and Cellular Structures. *Biofabrication* **2016**, *8* (2), 025016. https://doi.org/10.1088/1758-5090/8/2/025016.
17. Pedraza, E.; Brady, A.-C.; Fraker, C. A.; Stabler, C. L. Synthesis of Macroporous Poly(Dimethylsiloxane) Scaffolds for Tissue Engineering Applications. *J. Biomater. Sci. Polym. Ed.* **2013**, *24* (9), 1041–1056. https://doi.org/10.1080/09205063.2012.735097.
18. Hinton, T. J.; Hudson, A.; Pusch, K.; Lee, A.; Feinberg, A. W. 3D Printing PDMS Elastomer in a Hydrophilic Support Bath via Freeform Reversible Embedding. *ACS Biomater. Sci. Eng.* **2016**, *2* (10), 1781–1786. https://doi.org/10.1021/acsbiomaterials.6b00170.

19. Hinton, T. J.; Jallerat, Q.; Palchesko, R. N.; Park, J. H.; Grodzicki, M. S.; Shue, H.-J.; Ramadan, M. H.; Hudson, A. R.; Feinberg, A. W. Three-Dimensional Printing of Complex Biological Structures by Freeform Reversible Embedding of Suspended Hydrogels. *Sci. Adv.* **2015**, *1* (9), e1500758–e1500758. https://doi.org/10.1126/sciadv.1500758.

20. Bingham plastic model - Schlumberger Oilfield Glossary https://www.glossary.oilfield.slb.com/en/Terms/b/bingham_plastic_model.aspx (accessed Nov15, 2018).

Chapter III

Materials and Methods

This Chapter aims to provide relevant information that are not present in the 4th practical chapter, including materials properties and chemical functionalization, processing technology description, optimization of the printed parameters and biological assays used for the development of a functional support bath for the 3D bioprinting of freeform hybrid structures. Supplier specifications can be found in the experimental subsection of the following chapter.

1. Materials

The work of this master thesis is mainly focused on the 3D bioprinting of alginate hydrogels within a novel support bath based on xanthan gum derivatives. Therefore, alginate and xanthan gum are the major materials exploited in the present work. A more detailed information concerning their specific properties is provided below.

1.1. Alginate

Alginate is naturally occurring anionic and hydrophilic polysaccharides obtained from brown seaweed [1]. This marine-based polysaccharide is a branched copolymer composed of alternating blocks of α-L-guluronic acid (G) and β-D-mannuronic acid (M) units linked by type 1→4 glycosidic linkages, composition and broadly variable sequence structure [2]. Alginate is probably the most widely used hydrogel 3D structures constructs due to its biodegradability, low toxicity, biocompatibility and its fast and reversible ability to crosslink into hydrogels in the presence of divalent cations, namely calcium ions [1]. Since the number and arrangement of G blocks define the stability of the formed gels, that is, the higher the G-unit content, the more stability the gel will have [2]. In general, the gelation mechanism is based on intra- and intermolecular reactions of Ca^{2+} with the alginate molecules, forming cross-links between the carboxyl groups and the calcium ions. This phenomenon was described by Grant el al., and became known as the "egg-box" model [3].

More information on alginate properties and applications as a biomaterial can be found in Chapter 1.

1.2. Xanthan gum

Xanthan gum is a water soluble anionic extracellular polysaccharide obtained by carbohydrates fermentation from a phytopathogenic bacterium of the genus Xanthomonas. It was discovered in the 1950s at the Northern Regional Research Laboratories (NRRL) of the United States [3].

In 1969, xanthan gum was approved by the FDA (Food and Drug Administration), being applied to numerous products in different industrial segments, among them, food, pharmaceuticals, cosmetics, chemical [4,5]. The high industrial interest in this polysaccharide is mainly due to its rheological properties (shear thinning behavior), which allow the formation of viscous solutions at low concentrations (0.05- 1.0%) and their stability over a wide pH range (2.5 <pH > 11) and temperature (10°C to 90°C).

Regarding the chemical structure, xanthan gum backbone consists of a primary chain of β-D-(1,4)-glucose unit blocks, witch has a branching trisaccharide side chain. The branched side contains both glucuronic acid and pyruvic acid groups that confers the anionic character to the polysaccharide (figure 3.1) [6,7]. Moreover, the large number of hydroxyl and carboxyl moieties represents an elegant strategy to introduce functional groups for novel materials design approaches.

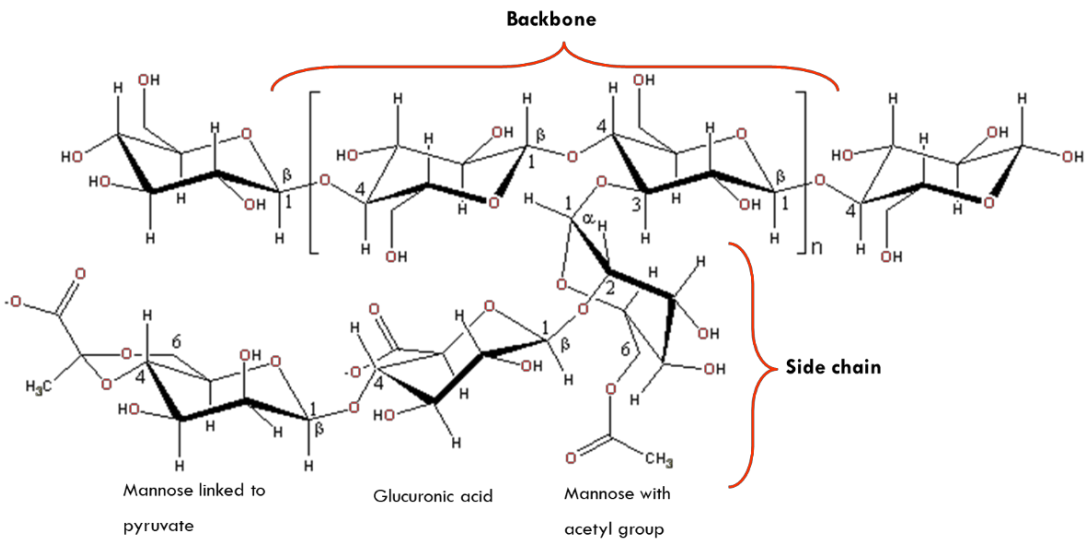

Figure 3.1. Chemical structure of Xanthan Gum.

The solutions of xanthan gum exhibit a highly pseudoplastic behaviour (shear thinning), which depends on temperature, salt concentration, pH and xanthan concentration. The apparent viscosity decreases as the shear rate increases, and this behaviour is called roughing or pseudoplasticity. However, these solutions are not thixotropic, which means that after high shear the initial viscosity is rebuilt instantly [8].

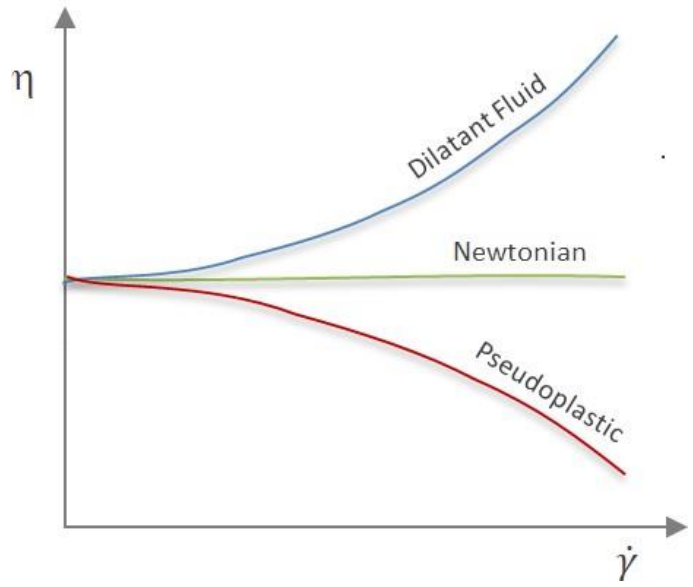

Figure 3.2. Rheology of non-newtonian fluids [9].

In recent years, the use of XG has grown considerably in several areas. Due to its characteristics, including biocompatibility and biodegradability, this gum is ideal to produce polymeric biomaterials for various medical applications, such as the controlled release of drugs [10] and tissue engineering [11,12,13].

1.3. Synthesis of glycidyl methacrylate xanthan gum

The introduction of methacrylic pendant groups into the backbone of natural based polymers is a common and simple approach in tissue engineering applications to create photocrosslinkable 3D hydrogels networks [14,15,16] These specific unsaturated functional groups (e.g. acrylates) undergo free radical polymerization in the presence of a photoinitiator upon ultraviolet (UV) irradiation. For the purpose of constructing a perfusable hydrogel support (Chapter 4), xanthan gum with methacrylic groups was functionalized based on the procedure reported by Huang and co-worker[17]. The synthetic route is depicted in figure 3.3.

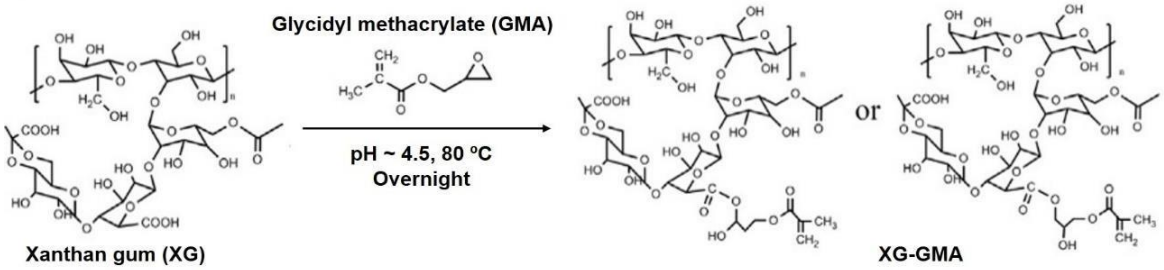

Figure 3.3. Schematic representation of the synthesis of XG-GMA. Adapted from reference[17].

2. Cell sources

Cell lines are very useful for research as they provide reliable experimental results because of the possibility of obtaining large amounts of cells for prolonged use. In the present thesis were used a mouse fibroblasts L929 Cell Line (European Collection of Authenticated Cell Cultures (ECCC), United Kingdom). L929 fibroblast cell lines is one of the most widely used cell lines in many standard tests, such as in biocompatibility tests, drug cytotoxicity testing, and in biology studies[18].

3. Material processing

3.1. Envisiontec Bioplotter

The 3D-Bioplotter® System from Envisiontec is a Rapid Prototyping tool, used since 2000 to process a wide variety of biomaterials in the Tissue Engineering process. This machine has a lot of specifications, some of them are described in the table below (table 3.1).

Table 3.1. Specifications of the 3D-Bioplotter® developer series[19].

Axis Resolution (XYZ)	0.001 mm (0.00004")
Speed	0.1 - 150 mm/s (0.004" - 5.91"/s)
Pressure	0.1 - 9.0 bar (1.45 - 130 psi)
Build Volume (XYZ)	150 x 150 x 140 mm (5.91" x 5.91" x 5.51")
Needle Position Control	Photo Sensor
Camera Resolution (XY)	-
Needle Sensor Resolution (XYZ)	0.03 mm (0.0012")
Minimum Strand Diameter	0.100 mm (0.004") - Material Dependent
Number of Materials per Scaffold	Maximum 3 Materials using 3 Print Heads
Print Heads Included	1x Low and 1x High Temperature Head
Filters Included	Particle and Sterile Filters
Platform Temperature Control	Heating and Cooling Capable (Chiller not included)
Platform Height Control	Automatic Z-height Controlling System
Material Calibration	Manual Material Calibration
Additional Features	Automated Nozzle Cleaning Process
	-
	-

The 3D-Bioplotter system imports 3D CAD models and fabricates physical 3D scaffolds with the outer form defined by the model's data and a complex inner structure with a user-designed interconnectivity porosity (figure 3.4).

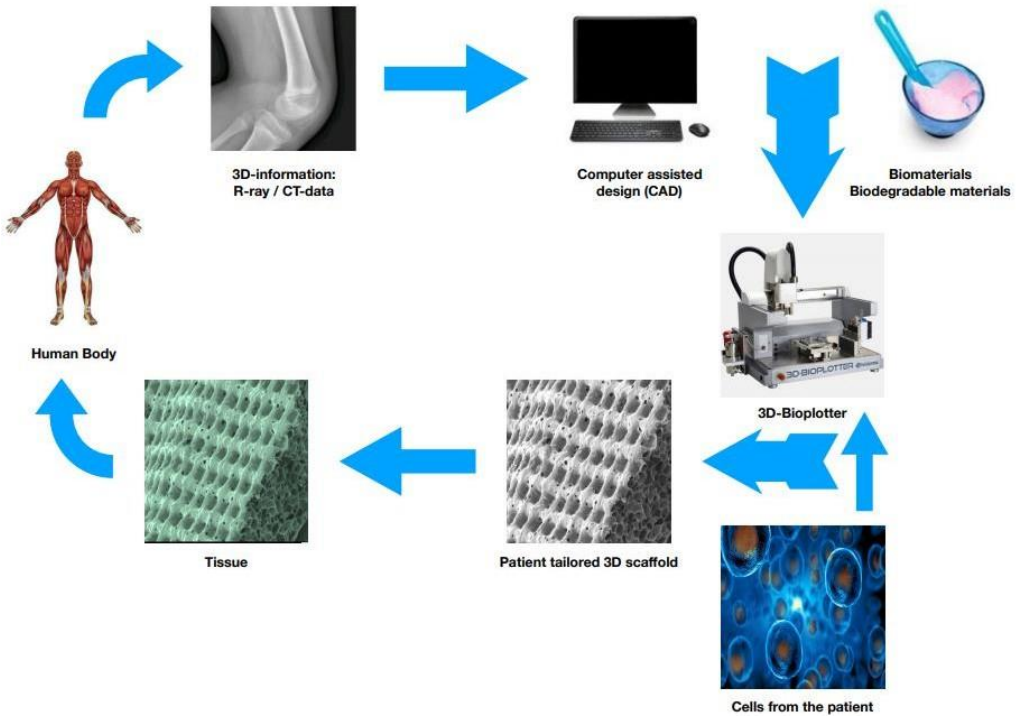

Figure 3.4. Process chain for computer aided tissue engineering.

The key point of this technique is the capability to process a wide range of materials from any unique RP machine, from soft hydrogels over polymers to ceramics and hard metals.

There are three fundamental steps required for production using 3D-Bioplotter®, also shown schematically in figure 3.5:

• Computer-aided design (CAD): Every part to be produced by additive manufacturing must have its geometry defined by a numerical model (software).
• Conversion to STL: The digital model is usually stored in STL format using a triangular or Cartesian representation of the model. This STL file only describes the surface of a 3D volume without information about its internal space.
• Transfer to the additive manufacturing machine and file manipulation: From this STL format, a machine code is generated, called the programming language G (G Code). Afterwards, the STL file is computationally sliced into hundreds - sometimes thousands - of thin 2D horizontal layers. The 3D printer then reads these 2-D layers as building blocks and deposit them in successive layers, thus forming a three-dimensional object. In this step we can correct the positioning, size or orientation of the part.

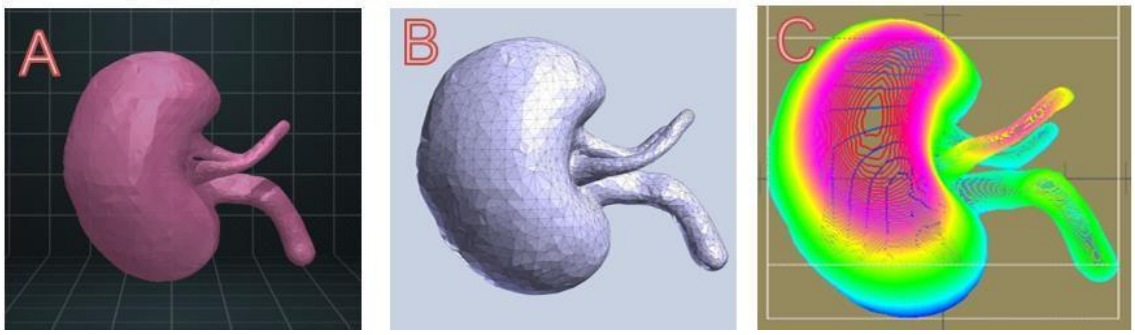

Figure 3.5. Sequential steps involved in a 3D printing process. (A) Designed 3D Computer aided design (CAD); (B) Stereolithography (STL) file of the model; (C) Slicing or 3D printing software.

Before starting to print, it is necessary to set some parameters in the machine, such as the thickness of the layers, the distance between layers, how far from the base we want to start printing among others. And another import step is the choice of needle.We use a smoothflow tapered tip with 25g.

On the material editor tab an overview of all saved low and high temperature material is displayed. Each material can be selected, and the corresponding parameters

changed. Under Basic Parameters the values for temperature (2ºC-250ºC), Pressure (0,1 bar-9,5 bar) and speed (0,1-150mms^{-1}) in X and Y cab be set. Table 3.2 shows the parameters used in this work.

Table 3.2. Parameters of alginate hydrogel.

Parameters	
Temperature	20ºC
Pressure	0,3 bar
Speed	30 mm/s
Density	1,00 g/cm^3
Minimum lenght	3,00 mm

Having defined all these parameters, we can move on to printing. This process is fully automated with a low need for direct human supervision, it is only necessary to guarantee the supply of materials, the discharge of the machine and to prevent / act on eventual problems.

Bioprinting with 3D-Bioplotter allows researchers a wide range of materials (cells, gels, fibers, polymers, ceramics, metals) in a single scaffolding object that can replace tissues and organs that are damaged or missing.

Biofabrication research is being done in a wide range of areas, with a wide range of materials. Some works of applications of biofabrication technique are described in the table below (table 3.3).

Table 3.3. Applications of Biofabrication technique in Bone regeneration [20,21,22,23], Drug Release [24,25,26,27,28], Soft tissue/ Cartilage Fabrication and Cell Printing/ Organ Printing [29,30,31,32,33,34] and 4D Printing and other applications [35,36,37,38]

Bone Regeneration	Ceramic/Metal pastes	Hidroxyapatite	Titanium	Tricalcium Phosphate		
	Thermoplasts	PCL	PLLA	PLGA		
Drug Release	Thermoplasts	PCL	PLLA	PLGA		
Soft tissue Cartilage Fabrication Cell and organ Printing	Hydrogels	Agar	Gelatin	Soy	Hyaluronic acid	Alginate	Chitosan
4D Printing and other applications	Other Materials	Acrylates	Silicone	Graphene	Polyurethane		

3.2. Optimization of the printing process conditions

All alginate hydrogels formulations were loaded into 30 ml syringes fitted with 22G needle and allowed to equilibrate to the surrounding temperature of 20 ºC before printing. Each filament was obtained by printing a single layer. After 1h, printed hydrogels were placed in ultrapure water and observed by optical microscopy after 24h. Images were acquired with the ZEN program and the strand diameter was estimated by ImageJ software (n =3 measurement per each image).

3.2.1. Materials concentrations

3.2.1.1. Xanthan gum

Xanthan gum has a good water solubility but requires vigorous stirring to avoid the formation of lumps. In this work, XG concentrations varied from 0.5 to 2.0% (w/v) were investigated in order to define the best one for the support bath. A significant increase in the liquid viscosity was observed above 1.0% XG concentration. However, for concentration higher than 1.5%, lumps formation was clearly observed. In this context, the optimum concentration of XG was found to be 1.5% (w/v). To prove the ability to support alginate hydrogels, an ALG filament was extruded through a 25G needle gauge within a flask containing 1.5% (w/v) of XG. It was observed that, upon extrusion, the filament did not disperse through the solution, remaining stable over time. Furthermore, to evaluate the shear thinning behavior, XG 1.5% (w/v) response to shear were examined in continuous flow experiments with a linearly ramped shear rate from 10^{-2} to 100 s^{-1}. As shown in figure 3.6, the viscosity of XG 1.5% (w/v) decrease linearly with increasing the shear rate due to the shear-induced reorganization of the polymer chains to a more stretched conformation. This response clearly demonstrates the shear-thinning behavior of the XG solution.

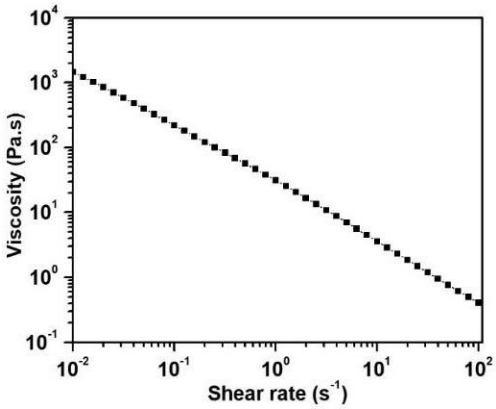

Figure 3.6. Viscosity variation as a function of shear rate for 1.5% (w/v) XG solution.

3.2.1.2. Calcium chloride and alginate

The alginate hydrogel printed diameter as a function of the alginate and calcium chloride (ionic crosslinker) concentrations was investigated. Generally, the filament sizes decrease by increasing both alginate and $CaCl_2$ concentrations (Figure 3.7), reaching the lowest filament thickness, without dragging and that can be easily handled after removing from the bath.

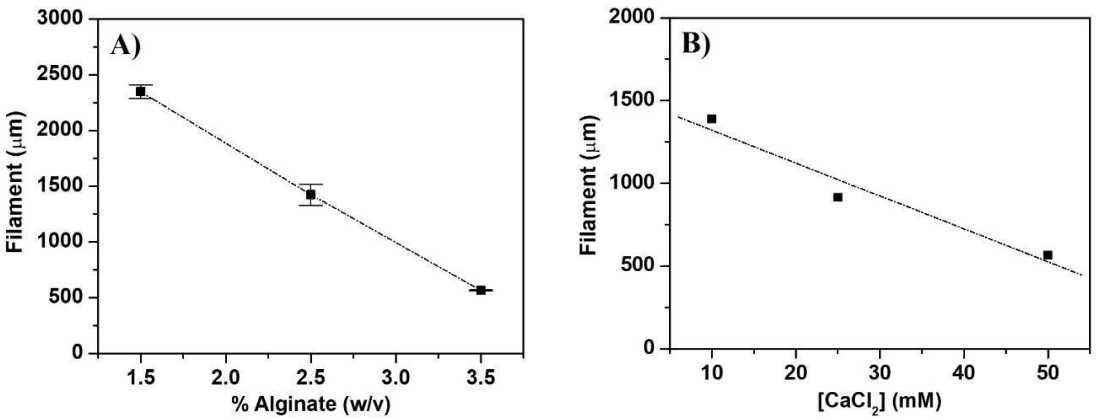

Figure 3.7. Quantification (moving speed 20 mms^{-1} and 0.4 bar) under different concentrations of **A)** alginate solution (50 mM of $CaCl_2$ within the XG support bath) and **B)** $CaCl_2$ within the XG support bath under a constant ALG concentration (3.5% w/v).

3.3. Effect of the pressure and speed print parameters on the printed filament sizes

The influence of printing parameters on the alginate hydrogel printed strands diameter was also investigated by varying the deposition speed (i.e., 10, 15, 20, 25, 30 and 35 mms^{-1}) and extrusion pressure (i.e., 0.2, 0.4 and 0.6 bar), for a total of 18 combinations (figure 3.8).

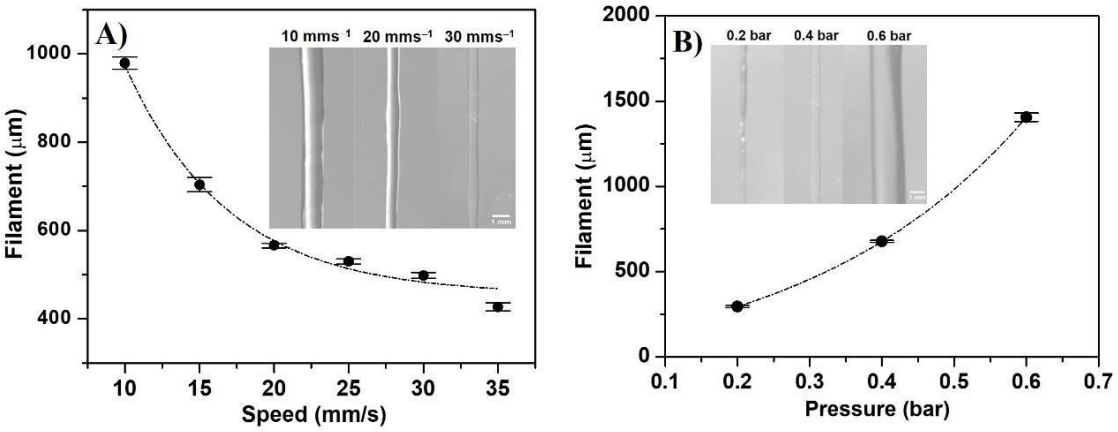

Figure 3.8. Characterization of printed filaments (3.5 % w/v ALG hydrogel, 50 mM $CaCl_2$ in XG support bath): **A)** Filament sizes with variations in moving speed under fixed extrusion pressure (0.4 bar) and **B)** Filament sizes as a function of the extrusion pressure under constant moving speed (30 mms^{-1}).

Under a constant extrusion pressure of 0.4 bar, the filament size decreases as the needle's speed increase, ranging from 1 mm to 400 µm. However, for moving speeds higher than 30 mms^{-1}, the ability to print continuous thinner filaments decreases because of the diameter needle.

When the needle's speed is kept constant (20 mms^{-1}), the size of the printed filaments increases significantly with the extrusion pressure because of the extrusion flux increase. For low values as 0.2 bar, the filaments are so thin, being difficult to remove them from the support bath after ionic crosslinking. Moreover, the low extrusion pressure also causes the alginate hydrogel drawn the XG bath. In this context, it was defined that the best moving speed and extrusion pressure are 30 mms^{-1} and 0.3 bar, respectively.

3.4. 3D Printing of freeform suspended structures

Freeform suspended structures were produced by three-dimensional plottingmethod (3DP) method using a 3D Bioplotter system (4th generation, EnvisionTec GmbH).3D printed structures were designed using the CAD programme (SolidWorks). The CAD files were then converted to STL files and transferred to the relative software to generate printing paths. The alginate solution was loaded into the extrusion syringes and then nozzles with 0.25 mm fitted to the end of syringes. When the sol phase was attained, a nitrogen gas pressure of 0.3 bar was applied to the syringe through a pressurized cap. The plotting speed was set as 30 mms^{-1} and the spacing between two deposited fibers was 200 µm. To maintain the shape of the deposited fibers and the structure of the whole scaffolds, the alginate was extruded within a XG support bath containing 50 mM of $CaCl_2$ in order to promote the quickly ionic gelation of alginate (see Figure 5)

At the end, structures were air-dried within the XG support bath, at ambient conditions for 24 h. Thereafter the structures are withdrawn from the bath and washed in distilled water.

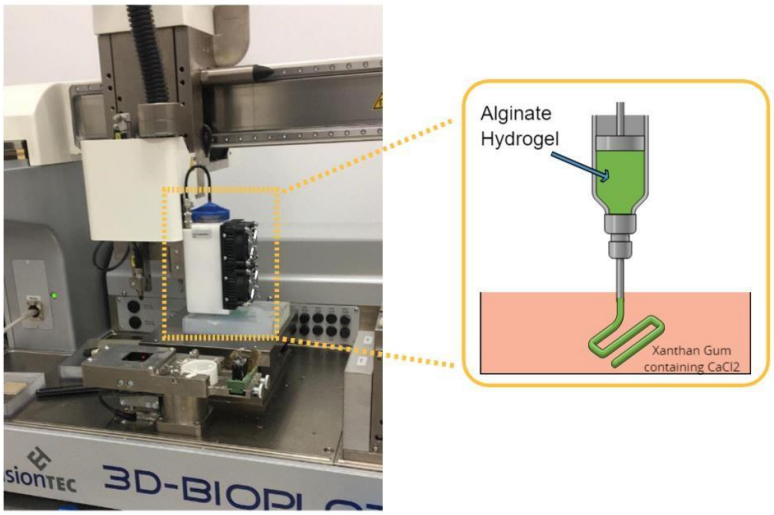

Figure 3.9. Schematic of the printing process using a 3D bioplotting technique supplemented with a submerged cross-linking process

3.5. In vitro cell culture

3.5.1. Cell-laden bioink preparation and 3D-printing

The bioprinting process was performed after an accurate disinfection of the 3D printer with 70% w/v ethanol solution and sterilization all the material by UV irradiation.

The biological performance of alginate hydrogels in a liquid medium was assessed using the L929 Cell Line (European Collection of Authenticated Cell Culture, United Kingdom). L929 cells were seeded in T-flasks 175 cm^2 using Dulbecco's Modified Eagle's Medium Low Glucose (DMEM-LG), supplemented with 10% (v/v) fetal bovine serum and (1% (v/v) antibiotic/antimycotic in controlled atmosphere of 5% CO_2, 95% relative humidity and 37°C. After reach confluence, cells were trypsinized and resuspended in the alginate printing solution at a density of 8×10^6 cells/mL. The solution was then mixed using a stirring plate at 500 rpm for 5min at room temperature, before loading to the syringe.

3.5.2. Live/Dead cell assays

The presence of cells inside the 3D printed filament was analysed at the 3rd and 7th days. To evaluate the 3D printed filament cell viability, L929 cells were labelled with Acetomethoxy derivative of calcein (Calcein-AM) (2 μg/mL) and Propidium Iodide (PI) (1 μg/mL) for 30 min at 37 °C. Following incubation, the 3D filament was washed twice with DPBS and imaged immediately by fluorescence microscopy. Acquisition of fluorescence micrographs was performed in an upright widefield microscope (Axio Imager M2, Carl Zeiss, Germany), or in laser scanning confocal microscopes (LSM510 Meta, and LSM 880 Airyscan, Carl Zeiss, Germany).

4. Fabrication of a perfusable XG-based device

In order to create a multifunctional bath where it is possible to print asymmetric complex structures and remove them without collapsing, we also endeavour the possibility to photocrosslink the support bath at the end of the printing process and remove the printed structures by liquefying the alginate hydrogel with EDTA solution. This approach opens a

new gateway towards the 3D printing of vascularized constructs. In this sense, we firstly functionalized the XG with methacrylic moieties that are photocrosslinkable under UV light. A solution of 1% (w/v) XG-MA was prepared in PBS containing 0.5% (w/v) of irgacure I2959 and stirred overnight at room temperature (figure 3.10). An alginate filament with a wave form was printed within this XG-based support bath, using the optimizing printed parameters afore mentioned (pressure=0.3 bar, speed=30mms^{-1}). Afterwards, the support bath was exposed to UV light during 60 s (350-420 nm, 200 mW/cm^2), forming a photocrosslinked hydrogel. This one was immersed in an EDTA solution (20 mM), overnight in order to liquefy the alginate filament.

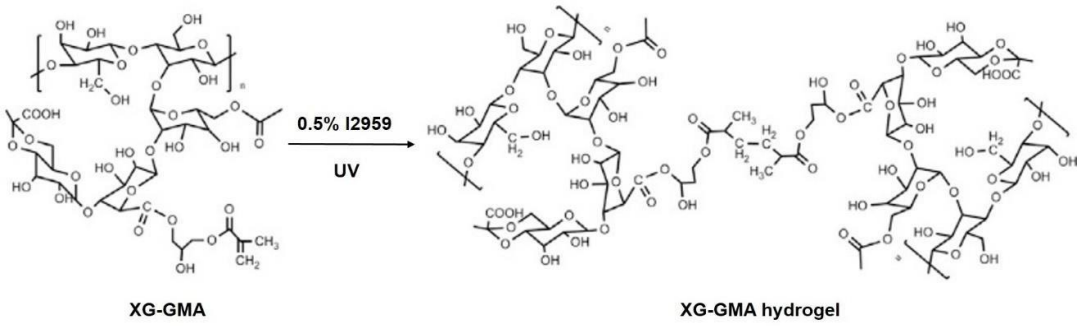

Figure 3.10. Schematic illustration of the photocrosslink XG-MA polymer in the presence of the irgacure photointiator to create XG-MA hydrogel networks.

5. References

1. Lee, K. Y.; Mooney, D. J. Alginate: Properties and Biomedical Applications. *Prog. Polym. Sci.* **2012**, *37* (1), 106–126. https://doi.org/10.1016/j.progpolymsci.2011.06.003.
2. Agüero, L.; Zaldivar-Silva, D.; Peña, L.; Dias, M. L. Alginate Microparticles as Oral Colon Drug Delivery Device: A Review. *Carbohydr. Polym.* **2017**, *168*, 32–43. https://doi.org/10.1016/J.CARBPOL.2017.03.033.
3. Margaritis, A.; Zajic, J. E. Mixing, Mass Transfer, and Scale-up of Polysaccharide Fermentations. *Biotechnol. Bioeng.* **1978**, *20* (7), 939–1001. https://doi.org/10.1002/bit.260200702.
4. Katzbauer, B. Properties and Applications of Xanthan Gum. *Polym. Degrad. Stab.* **1998**, *59* (1–3), 81–84. https://doi.org/10.1016/S0141-3910(97)00180-8.
5. Kumar, A.; Rao, K. M.; Han, S. S. Application of Xanthan Gum as Polysaccharide in Tissue Engineering: A Review. *Carbohydr. Polym.* **2018**, *180*, 128–144.

https://doi.org/10.1016/j.carbpol.2017.10.009.

6. Habibi, H.; Khosravi-Darani, K. Effective Variables on Production and Structure of Xanthan Gum and Its Food Applications: A Review. *Biocatal. Agric. Biotechnol.* **2017**, *10*, 130–140. https://doi.org/10.1016/J.BCAB.2017.02.013.
7. Wang, Z.; Wu, J.; Zhu, L.; Zhan, X. Characterization of Xanthan Gum Produced from Glycerol by a Mutant Strain Xanthomonas Campestris CCTCC M2015714. *Carbohydr. Polym.* **2017**, *157*, 521–526. https://doi.org/10.1016/j.carbpol.2016.10.033.
8. Garcõ Âa-Ochoa, F.; Santos, V. E.; Casas, J. A.; Go Âmez, E. *Xanthan Gum: Production, Recovery, and Properties*.
9. rheologyhttp://www1.lsbu.ac.uk/php-cgiwrap/water/pfp.php3?page=http://www1.lsbu.ac.uk/water/rheology.html (accessed Nov 26, 2018).
10. Jian, H.; Zhu, L.; Zhang, W.; Sun, D.; Jiang, J. Galactomannan (from Gleditsia Sinensis Lam.) and Xanthan Gum Matrix Tablets for Controlled Delivery of Theophylline: In Vitro Drug Release and Swelling Behavior. *Carbohydr. Polym.* **2012**, *87* (3), 2176–2182. https://doi.org/10.1016/j.carbpol.2011.10.043.
11. Mei, L.; Shen, B.; Xue, J.; Liu, S.; Ma, A.; Liu, F.; Shao, H.; Chen, J.; Chen, Q.; Liu, F.; et al. Adipose Tissue–derived Stem Cells in Combination with Xanthan Gum Attenuate Osteoarthritis Progression in an Experimental Rat Model. *Biochem. Biophys. Res. Commun.* **2017**, *494* (1–2), 285–291. https://doi.org/10.1016/J.BBRC.2017.10.039.
12. Petri, D. F. S. Xanthan Gum: A Versatile Biopolymer for Biomedical and Technological Applications. *J. Appl. Polym. Sci.* **2015**, *132* (23), n/a-n/a. https://doi.org/10.1002/app.42035.
13. Kumar, A.; Rao, K. M.; Han, S. S. Development of Sodium Alginate-Xanthan Gum Based Nanocomposite Scaffolds Reinforced with Cellulose Nanocrystals and Halloysite Nanotubes. *Polym. Test.* **2017**, *63*, 214–225. https://doi.org/10.1016/j.polymertesting.2017.08.030.
14. Coutinho, D. F.; Sant, S. V.; Shin, H.; Oliveira, J. T.; Gomes, M. E.; Neves, N. M.; Khademhosseini, A.; Reis, R. L. Modified Gellan Gum Hydrogels with Tunable Physical and Mechanical Properties. *Biomaterials* **2010**, *31* (29), 7494–7502. https://doi.org/10.1016/j.biomaterials.2010.06.035.
15. Custódio, C. A.; Reis, R. L.; Mano, J. F. Photo-Cross-Linked Laminarin-Based Hydrogels for Biomedical Applications. *Biomacromolecules* **2016**, *17* (5), 1602–1609. https://doi.org/10.1021/acs.biomac.5b01736.
16. Babo, P. S.; Pires, R. L.; Santos, L.; Franco, A.; Rodrigues, F.; Leonor, I.; Reis, R. L.; Gomes, M. E. Platelet Lysate-Loaded Photocrosslinkable Hyaluronic Acid Hydrogels for Periodontal Endogenous Regenerative Technology. *ACS Biomater. Sci. Eng.* **2017**, *3* (7), 1359–1369. https://doi.org/10.1021/acsbiomaterials.6b00508.
17. Huang, J.; Li, Z.; Hu, Q.; Chen, G.; Ren, Y.; Wu, X.; Ren, J. Bioinspired Anti-Digestive Hydrogels Selected by a Simulated Gut Microfluidic Chip for Closing Gastrointestinal Fistula. **2018**. https://doi.org/10.1016/j.isci.2018.09.011.
18. Theerakittayakorn, K.; Bunprasert, T. Differentiation Capacity of Mouse L 929 Fibroblastic Cell Line Compare With Human Dermal Fibroblast. 2012.

19. 3D Printers | Desktop, Professional and Industrial | EnvisionTEC https://envisiontec.com/ (accessed Dec 2, 2018).

20. Li, J. P.; de Wijn, J. R.; van Blitterswijk, C. A.; de Groot, K. The Effect of Scaffold Architecture on Properties of Direct 3D Fiber Deposition of Porous Ti6Al4V for Orthopedic Implants. *J. Biomed. Mater. Res. Part A* **2010**, *92A* (1), 33–42. https://doi.org/10.1002/jbm.a.32330.

21. Haberstroh, K.; Ritter, K.; Kuschnierz, J.; Bormann, K.-H.; Kaps, C.; Carvalho, C.; Mülhaupt, R.; Sittinger, M.; Gellrich, N.-C. Bone Repair by Cell-Seeded 3D-Bioplotted Composite Scaffolds Made of Collagen Treated Tricalciumphosphate or Tricalciumphosphate-Chitosan-Collagen Hydrogel or PLGA in Ovine Critical-Sized Calvarial Defects. *J. Biomed. Mater. Res. Part B Appl. Biomater.* **2010**, *93B* (2), 520–530. https://doi.org/10.1002/jbm.b.31611.

22. Jakus, A. E.; Rutz, A. L.; Jordan, S. W.; Kannan, A.; Mitchell, S. M.; Yun, C.; Koube, K. D.; Yoo, S. C.; Whiteley, H. E.; Richter, C.-P.; et al. Hyperelastic "Bone": A Highly Versatile, Growth Factor–free, Osteoregenerative, Scalable, and Surgically Friendly Biomaterial. *Sci. Transl. Med.* **2016**, *8* (358), 358ra127-358ra127. https://doi.org/10.1126/scitranslmed.aaf7704.

23. Kunjin, H.; Zeyu, Z.; Rongli, Z. Design of Orthopedic Plates and Its Modification Based On. *MCB Mol. Cell. Biomech.* **2016**, *12* (4), 265–286. https://doi.org/10.3970/MCB.2017.014.123.

24. Chateauvieux, S.; Morceau, F.; Dicato, M.; Diederich, M. Molecular and Therapeutic Potential and Toxicity of Valproic Acid. *J. Biomed. Biotechnol.* **2010**, *2010*, 1–18. https://doi.org/10.1155/2010/479364.

25. Yilgor, P.; Yilmaz, G.; Onal, M. B.; Solmaz, I.; Gundogdu, S.; Keskil, S.; Sousa, R. A.; Reis, R. L.; Hasirci, N.; Hasirci, V. An *in Vivo* Study on the Effect of Scaffold Geometry and Growth Factor Release on the Healing of Bone Defects. *J. Tissue Eng. Regen. Med.* **2013**, *7* (9), 687–696. https://doi.org/10.1002/term.1456.

26. Siyawamwaya, M.; du Toit, L. C.; Kumar, P.; Choonara, Y. E.; Kondiah, P. P. P. D.; Pillay, V. 3D Printed, Controlled Release, Tritherapeutic Tablet Matrix for Advanced Anti-HIV-1 Drug Delivery. *Eur. J. Pharm. Biopharm.* **2018**. https://doi.org/10.1016/j.ejpb.2018.04.007.

27. Zhu, M.; Li, K.; Zhu, Y.; Zhang, J.; Ye, X. 3D-Printed Hierarchical Scaffold for Localized Isoniazid/Rifampin Drug Delivery and Osteoarticular Tuberculosis Therapy. *Acta Biomater.* **2015**, *16*, 145–155. https://doi.org/10.1016/j.actbio.2015.01.034.

28. Zhang, J.; Zhao, S.; Zhu, M.; Zhu, Y.; Zhang, Y.; Liu, Z.; Zhang, C. 3D-Printed Magnetic Fe_3O_4/MBG/PCL Composite Scaffolds with Multifunctionality of Bone Regeneration, Local Anticancer Drug Delivery and Hyperthermia. *J. Mater. Chem. B* **2014**, *2* (43), 7583–7595. https://doi.org/10.1039/C4TB01063A.

29. Billiet, T.; Gevaert, E.; De Schryver, T.; Cornelissen, M.; Dubruel, P. The 3D Printing of Gelatin Methacrylamide Cell-Laden Tissue-Engineered Constructs with High Cell Viability. *Biomaterials* **2014**, *35* (1), 49–62. https://doi.org/10.1016/J.BIOMATERIALS.2013.09.078.

30. Cengiz, I. F.; Pitikakis, M.; Cesario, L.; Parascandolo, P.; Vosilla, L.; Viano, G.; Oliveira, J. M.; Reis, R. L. Building the Basis for Patient-Specific Meniscal Scaffolds: From Human Knee MRI to Fabrication of 3D Printed Scaffolds. *Bioprinting* **2016**, *1–2*, 1–10.

https://doi.org/10.1016/J.BPRINT.2016.05.001.

31. Laronda, M. M.; Rutz, A. L.; Xiao, S.; Whelan, K. A.; Duncan, F. E.; Roth, E. W.; Woodruff, T. K.; Shah, R. N. A Bioprosthetic Ovary Created Using 3D Printed Microporous Scaffolds Restores Ovarian Function in Sterilized Mice. *Nat. Commun.* **2017**, *8*, 15261. https://doi.org/10.1038/ncomms15261.

32. Wang, M.-D.; Zhai, P.; Schreyer, D. J.; Zheng, R.-S.; Sun, X.-D.; Cui, F.-Z.; Chen, X.-B. Novel Crosslinked Alginate/Hyaluronic Acid Hydrogels for Nerve Tissue Engineering. *Front. Mater. Sci.* **2013**, *7* (3), 269–284. https://doi.org/10.1007/s11706-013-0211-y.

33. Izadifar, Z.; Chang, T.; Kulyk, W.; Chen, X.; Eames, B. F. Analyzing Biological Performance of 3D-Printed, Cell-Impregnated Hybrid Constructs for Cartilage Tissue Engineering. *Tissue Eng. Part C. Methods* **2016**, *22* (3), 173–188. https://doi.org/10.1089/ten.TEC.2015.0307.

34. Costantini, M.; Idaszek, J.; Szöke, K.; Jaroszewicz, J.; Dentini, M.; Barbetta, A.; Brinchmann, J. E.; Święszkowski, W. 3D Bioprinting of BM-MSCs-Loaded ECM Biomimetic Hydrogels for *in Vitro* Neocartilage Formation. *Biofabrication* **2016**, *8* (3), 035002. https://doi.org/10.1088/1758-5090/8/3/035002.

35. Kiziltay, A.; Marcos-Fernandez, A.; San Roman, J.; Sousa, R. A.; Reis, R. L.; Hasirci, V.; Hasirci, N. Poly(Ester-Urethane) Scaffolds: Effect of Structure on Properties and Osteogenic Activity of Stem Cells. *J. Tissue Eng. Regen. Med.* **2015**, *9* (8), 930–942. https://doi.org/10.1002/term.1848.

36. Bakarich, S. E.; Gorkin, R.; Panhuis, M. in het; Spinks, G. M. 4D Printing with Mechanically Robust, Thermally Actuating Hydrogels. *Macromol. Rapid Commun.* **2015**, *36* (12), 1211–1217. https://doi.org/10.1002/marc.201500079.

37. Nathan-Walleser, T.; Lazar, I.-M.; Fabritius, M.; Tölle, F. J.; Xia, Q.; Bruchmann, B.; Venkataraman, S. S.; Schwab, M. G.; Mülhaupt, R. 3D Micro-Extrusion of Graphene-Based Active Electrodes: Towards High-Rate AC Line Filtering Performance Electrochemical Capacitors. *Adv. Funct. Mater.* **2014**, *24* (29), 4706–4716. https://doi.org/10.1002/adfm.201304151.

38. Jakus, A. E.; Secor, E. B.; Rutz, A. L.; Jordan, S. W.; Hersam, M. C.; Shah, R. N. Three-Dimensional Printing of High-Content Graphene Scaffolds for Electronic and Biomedical Applications. *ACS Nano* **2015**, *9* (4), 4636–4648. https://doi.org/10.1021/acsnano.5b01179.

Chapter IV

3D Bioprinting of complex structures in liquid medium

3D Bioprinting of complex structures in liquid medium

Sousa, L.[1], Oliveira, J.M.[2] and Mano, J.F.[1]

[1]Department of Chemistry, CICECO – Aveiro Institute of Materials, University of Aveiro, Campus Universitário de Santiago, 3810-193, Aveiro, Portugal

[2] Escola Superior Aveiro Norte, University of Aveiro, Parque do Cercal, 3720-509 Santiago de Riba-Ul, Oliveira de Azeméis, Portugal

Abstract

3D printing standard scaffolds using hydrogels has been subject of numerous studies over the years. Currently, the major challenge is still the fabrication of complex hydrogel with precisely structural control, in order to mimic anatomical and physiological features.

In this work, a viscous liquid medium based on xanthan gum was shown to be an ideal support bath to construct suspended and asymmetric alginate hydrogel structures without deformation or collapse, even after removal from the medium. Furthermore, preliminary biocompatibility tests using L929 fibroblast cells have clearly demonstrated the possibility to maintain cells alive in xanthan gum culture medium during the whole printing process and proliferate over 7 days. The versatility of xanthan gum was still demonstrated by creating a photocrosslinked xanthan gum-based hydrogel support for 3D printing a sacrificial alginate hydrogel, thus allowing to obtain perfused engineered constructs.

Keywords: 3D printing; suspended hydrogels; liquid medium; xanthan gum, perfusable constructs.

1. Introduction

Currently, known therapies based on organ and tissue transplants are widely used, however the lack of donors and the possible complications at the immune level make this strategy very limiting. So tissue engineering shows a great promise to get around all these obstacles by producing tissue structures capable of replacing a damaged or even missing tissue [1,2].

To imitate these structures, several techniques from biomaterials and living cells were developed [3]. Among these techniques, 3D bioprinting proved to be the most promising because of its ability to apply layer by layer a variety of biomaterials and cells with high print resolution to construct 3D structures [4].

Three dimensional (3D) bioprinting has a strong impact on tissue engineering, enabling the fabrication of complex 3D constructs that best represent tissues [5]. Despite the success of this technique, the production of scaffolds with good structural properties and biological functions remains a challenge, with biomaterials chosen and manufacturing techniques being used as the main critical points. The success of 3D bioprinting also depends on the characteristics of the materials used. These should be liquid enough to allow them to be extruded but at the same time elastic enough to retain the impression of complex three-dimensional structures. Among the various biomaterials, hydrogels are excellent candidates for bioinks.

Hydrogels are water insoluble and three-dimensional (3D) hydrophilic network systems with high water content, allowing easy transport of oxygen, nutrients and cellular metabolites. The hydrogels have received special attention for many biomedical applications, such as biocompatibility, biodegradation, its similarity to the extracellular matrix (ECM), both at the structural and compositional levels, as a platform for cell culture, as the cells can remain between the polymer chains within the hydrogels [6,7,8]. The source of hydrogels is usually natural or synthetic polymers [9]. Natural hydrogels are typically derived from marine organisms or algae and have explicit biomedical applications and properties, such as non-toxicity and biodegradability, but are soft materials, which makes them have little stability.

Alginate, a naturally occurring polysaccharide extracted from algae, has numerous characteristics that make it one of the most attractive polymers for tissue engineering.

Among its wide range of characteristics, its biocompatibility, its elastic properties, its low cost, its non-toxicity and the ability to promote cell proliferation [10,11].

The printing capacity of hydrogels is also strongly determined by the crosslinking condition [12]. One of the most commonly used methods is bioprinting in which the cross-linking is submerged, i.e., the hydrogel solution is deposited and gelled in a cross-linking medium.

However, it is also noted that hydrogels are soft materials able to collapse during printing process, in particular in the absence of a carrier bath, because of the gravity effect and low stiffness.

In order to overcome these major drawbacks, several approaches consisting on different support bath formulations have been reported in the literature. One of them was developed by Hinton et al.,[13] where it used a granular gel composed of gelatin microparticles, capable of retaining the structural integrity of the printed structures. However, the production of the blended gelatin microparticles is a time-consuming process, which represents a great disadvantage for a 3D printing scale-up. Bhattacharjee et al.,[14] also managed to bypass this structural problem by using a bath composed of Carbopol microgels. However, Carbopol has some cytotoxicity decreasing the viability of this carrier bath.

In this work, we describe a new liquid support bath based on xanthan gum, with rheological and biological characteristics ideal to support 3D printing complex and totally asymmetric hydrogel structures as well as to fabricate perfusable engineered constructs.

2. Experimental section

2.1. Materials

Calcium Chloride dihydrate and sodium alginate (Mw 10000-600000 g mol^{-1}, viscosity 350-550 mPas) were purchased from PanReac AppliChem (Darmstadt, Germany). Xanthan gum free of gluten was obtained at the commercial store Celeiro. Fluorescein 5(6)-isothiocyanate (FITC), rhodamine B isothiocyanate (RITC), dimethylsulfoxide (DMSO, 99.5%), 2-hydroxy-4’-(2-hydroxyethoxy)-2-methylpropiophenone (I2959, 98%), Dulbecco’s Modified Eagle’s Medium (DMEM) and an immortalized mouse fibroblast cell line (L929, European Collection of Authenticated Cell Cultures) were supplied by Sigma-

Aldrich. Dibutyltin dilaurate (95%) and glycidyl methacrylate (GMA, >95%) were purchased from TCI Chemicals, while pyridine was from Acros Organics. Fetal bovine serum (FBS), calcein AM and propidium iodide were obtained from Thermo Fisher Scientific. Dulbecco's Phosphate-Buffered Saline (DPBS) without calcium and magnesium was supplied by VWR.

2.2. Preparation of the xanthan gum liquid medium and hydrogel (bio)inks

To prepare the liquid medium, 50mM of $CaCl_2$ was firstly dissolved in distilled water. Afterwards, 1.5% (w/v) of xanthan gum was slowly added to avoid the formation of lumps and kept under vigorous stirring overnight. For the ink preparation, a 3.5 % (w/v) alginate was dissolved in distilled water with 0.1% (w/v) of food dye.

For the preparation of the bioink, L929 cells were seeded in T-flasks 175 cm^2 using Dulbecco's Modified Eagle's Medium Low Glucose (DMEM-LG), supplemented with 10% (v/v) fetal bovine serum and (1% (v/v) antibiotic/antimycotic in controlled atmosphere of 5% CO_2, 95% relative humidity and 37°C. After reach confluence, cells were trypsinized and resuspended in the alginate printing solution at a density of 8×10^6 cells/mL. The solution was then mixed using a stirring plate for 5min at room temperature, before loading to the syringe.

2.3. 3D printing of suspended hydrogels

Freeform suspended structures were produced by three-dimensional plotting method (3DP) method using a 3D Bioplotter system (4th generation, EnvisionTec GmbH). Firstly, 3D printed structures were designed using the CAD programme (SolidWorks). The CAD files were then converted to STL files and transferred to the relative software to generate printing paths. The partially alginate hydrogel was loaded into the extrusion syringes and then nozzles with 0.25 mm fitted to the end of syringes. When the sol phase was attained, a nitrogen gas pressure of 0.3 bar was applied to the syringe through a pressurized cap. The plotting speed was set as 30 mms^{-1} and the spacing between two deposited fibers was 200 μm. To maintain the shape of the deposited fibers and the structure of the whole scaffolds,

the fibers should solidify quickly after dispensing. At the end, structures were air-dried at ambient conditions for 24 h. Thereafter the structures are withdrawn from the bath and washed in distilled water.

2.4. Live/dead assays

The presence of cells inside the 3D printed filament was analysed at the 3rd and 7th days. To evaluate the 3D printed filament cell viability, L929 cells were labelled with Acetomethoxy derivative of calcein (Calcein-AM) (2 μg/mL) and Propidium Iodide (PI) (1 μg/mL) for 30 min at 37 °C. Following incubation, the 3D filament was washed twice with DPBS and imaged immediately by fluorescence microscopy. Acquisition of fluorescence micrographs was performed in an upright widefield microscope (Axio Imager M2, Carl Zeiss, Germany), or in laser scanning confocal microscopes (LSM510 Meta, and LSM 880 Airyscan, Carl Zeiss, Germany).

2.5. Fabrication of a perfusable xanthan gum device

Xanthan gum was chemically modified with glycidyl methacrylate as previously described in the literature [15]. Briefly, xanthan gum was dissolved at 0.5% (w/v) in distilled water under vigorous stirring, at room temperature during night. Afterwards, 2 mL of glycidyl methacrylate was added dropwise. The reaction was carried out at 80 ºC for 12h. At the end, XG-GMA was precipitated with ethanol and then dissolved in warm water. The solution was dialyzed against water using 6-8 kDa cutoff dialysis membranes, for 5 days (changing water 3 times per day). The resulting solution was frozen at -80º C followed by freeze-drying and stored at 4°C, until further use. The obtained XG-GMA was characterized by proton nuclear magnetic resonance (^{1}H NMR) and Fourier transformed infrared spectroscopy (FTIR-ATR). NMR spectra were recorded at 70º C on a Bruker Advance III 300 MHz spectrometer. FTIR spectra were obtained in a Brucker Tensor 27 spectrometer (256 scans, 4 cm^{-1} resolution). For 3D printing alginate hydrogel filaments, 1% (w/v) of XG-GMA was dissolved in a phosphate-buffered saline solution containing 0.5% w/v 2-hydroxy-4′-(2-hydroxyethoxy)-2-methylpropiophenone (I2959). After 3D printing the alginate filament within XG-GMA support bath, this one was exposed to UV light during 60

s (350-420 nm, 200 mW/cm^2), forming a photocrosslinked hydrogel. Finally, the hydrogel support bath was immersed in an EDTA solution (20 mM), overnight in order to liquefy the alginate filament.

3. Results and Discussion

3.1. Printing parameter optimization and characterization of the filaments

After optimizing the concentrations of the support bath and the alginate hydrogel (see materials and methods chapter, section 3.2.3), critical print parameters, which included the pressure exerted on the gel in the syringe and the printing speed, were studied through the printing of single filaments that were then analysed. The data of the filament diameters for each of the formulations are explicit in Fig 4.1. These results were obtained by controlling the printing speed and the extrusion pressure during the printing of a hydrogel paint at a constant temperature of 20°C. The extrusion speed is very important for the print quality. A wide range of speeds was tested ranging from 10mms^{-1} to 40mms^{-1}. The results showed that as we increase the speed of printing, the diameter of the filaments decreases, and they become more regular. However, at speeds greater than 30 mms^{-1}, the extrusion of the filament is compromised, since the surface tension is so high that the filaments creep in and become attached to the print nozzle. Thus, the speed of 30mms^{-1} is defined as the ideal one.

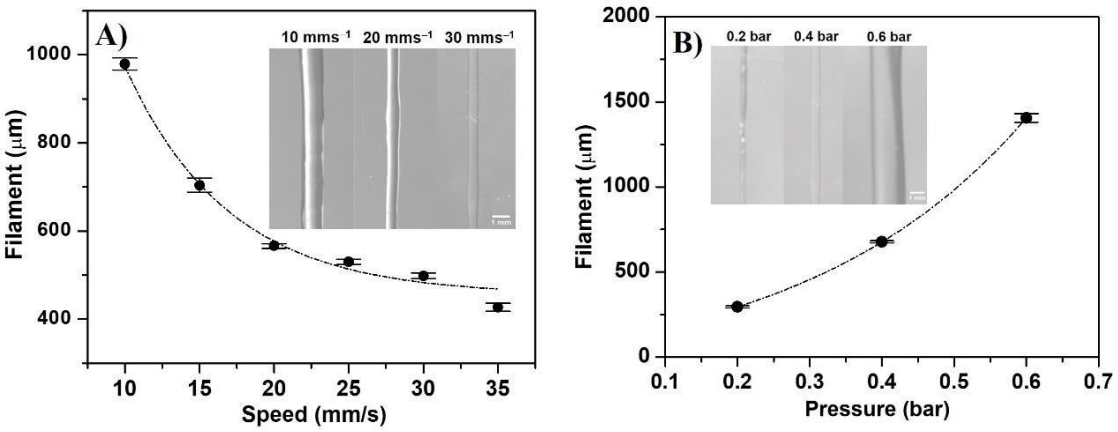

Figure 4.1. Characterization and visualization of printed filaments (3.5 % w/v ALG hydrogel, 50 mM $CaCl_2$ in XG support bath): **A)** Filament sizes with variations in moving speed under fixed extrusion pressure (0.4 bar) and **B)** Filament sizes as a function of the extrusion pressure under constant moving speed (30 mms^{-1}).

The extrusion pressure is also a very important parameter since it determines the extrusion output, which directly affects the width of the printed line. The pressure is determined by the viscosity of the printed materials. Extrusion under different pressures was also investigated. When we apply pressures below 0.2 bar, we cannot obtain any kind of extrusion, and even at 0.2 bar pressure the extruded filaments are so thin that they cannot be removed from the bath. At pressures over 0.6 bar the extrusion is very fast, the filaments are very thick and uneven, resulting in poor print quality. We then limit our studies to between 0.2 and 0.6 bar. However, thinner filaments require a shorter crosslinking time and allow the construction of thinner and more accurate structures. However, the extrusion pressure and the printing speed are not mutually independent, and a higher extrusion pressure can be compensated for by a faster printing speed. So, we combined the 2 printing parameters and got the following conditions as the ideas for our materials: extrusion temperature at 20°C, extrusion head speed at 30 mms^{-1} and extrusion pressure at 0.3 bar.

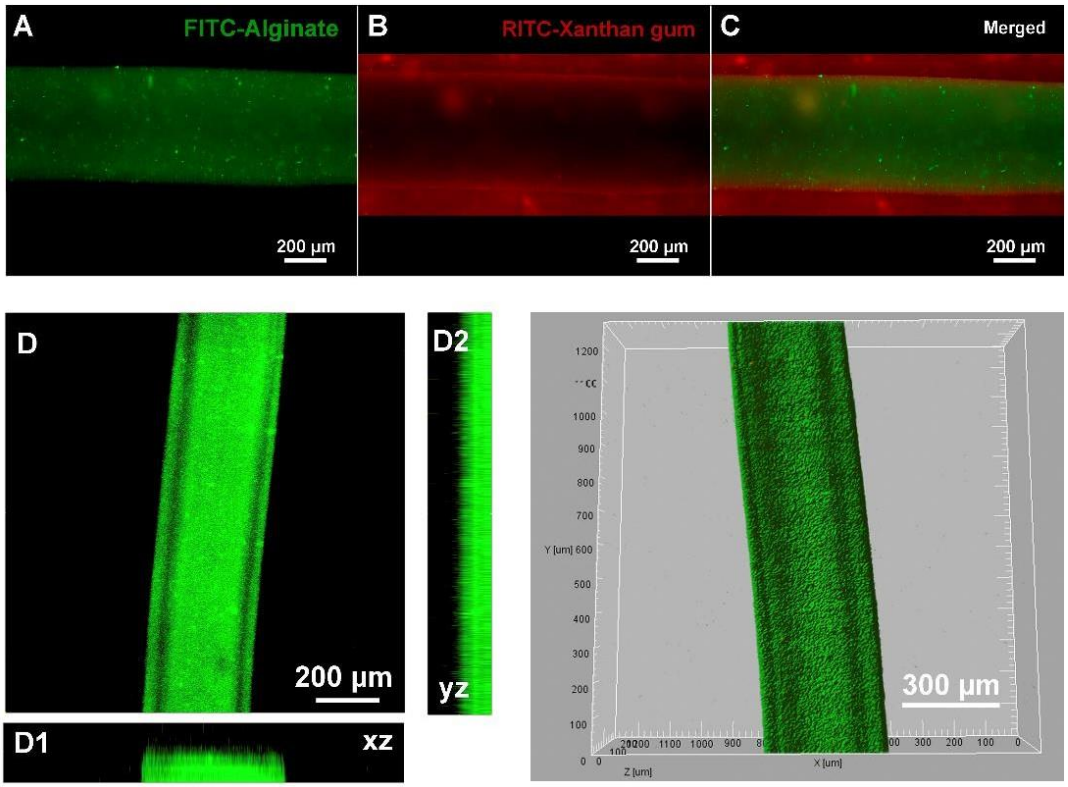

Figure 4.2. Fluorescence microscopy characterization of 3D filament: Alginate filament (FITC, green) (A), Xanthan gum printing support media (RITC, red) (B), Merging of the Filament channel and support media channel (C); Orthogonal projection of alginate 3D filament top view (D), frontal view (D1) and side view (D2); 3D reconstruction of alginate filament bottom view (E).

After defining the optimum printing parameters, we investigated the possibility of diffusion occurrence between both medium by labelling ALG and XG with different fluorochromes. According the figure 4.2, the quickly ionic gelation mechanism of ALG doesn't allow the mixture and ulterior diffusion between ALG hydrogel and XG support bath.

3.2. Development of a new support bath and its ability to freeform suspended hydrogels

Despite, 3D printing process consists on the standard layer-by-layer planar fabrication, we endeavour to demonstrate the potentiality of the xanthan gum support bath to sustain freeform extruded material in 3D space. This is clearly demonstrated in Figure 4.3 where is possible to observe a continuous extruded single filament moving simultaneous in all three axes without touching the previously deposited material. This is the proof-of-concept of the true freeform, since it is not limited to the standard layer-by-layer deposition.

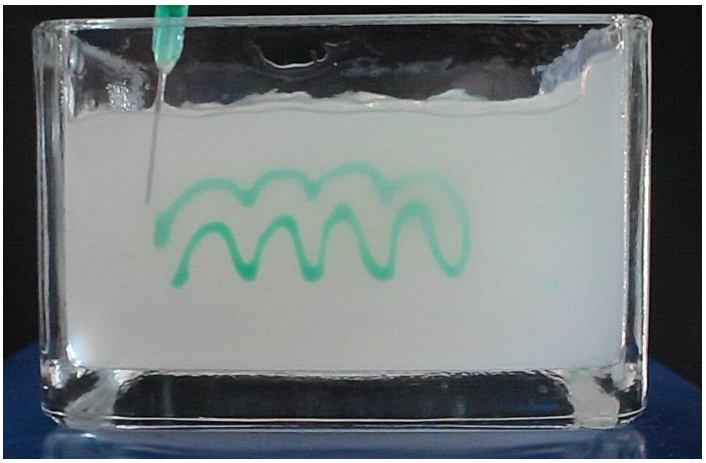

Figure 4.3. Free-form structure. Free drawing of an alginate structure in xanthan gum bath.

3.3. Writing asymmetric structures in liquid medium

To explore the stability of writing in xanthan gum liquid medium we have generated a completely asymmetric structure that printed without media would collapse, thus losing structural integrity. We then create a model of a vessel in which the centre of gravity does not coincide with the centre of the structure, with a layer spacing of 200μm and a base

distance of 0.5mm. In creating this structure, we prove that our bath has an immediate crosslinking ability, that is, as the layers are deposited there is crosslinking, allowing the adhesion of these and the consequent ability to print structures without interference of repeated movement of retraction of the extrusion head in the structure construction.

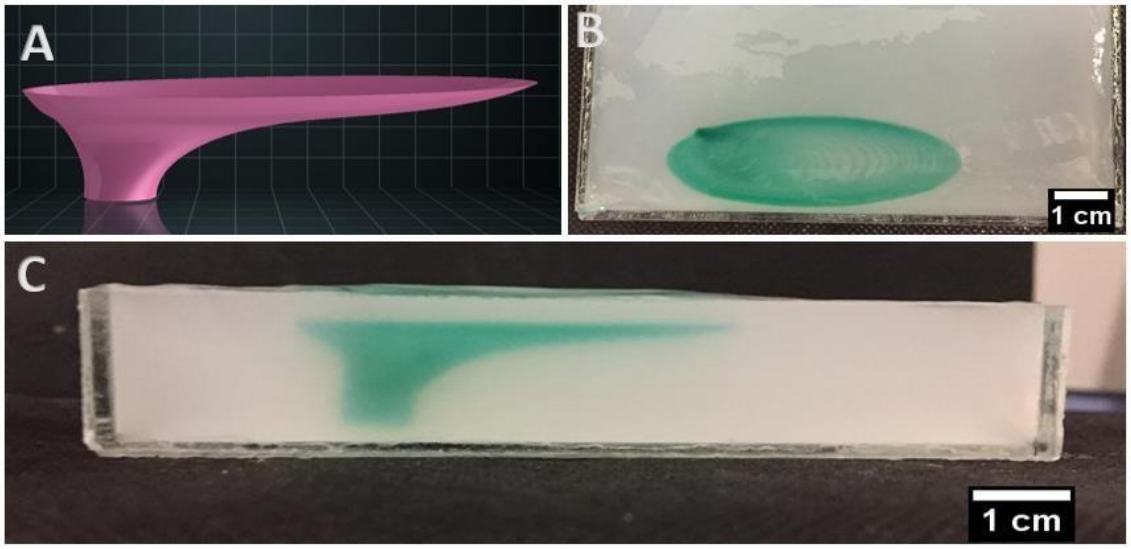

Figure 4.4. (A) 3D CAD model of the asymmetric structure; (B) Top view of the printed structure; (C) Front view of the printed asymmetric structure.

The fact that we start printing away from the container base allows us to show that the structure maintains its integrity without requiring any additional support. In the top-view (figure 4.4.B) images we show that the stability provided by the liquid medium allows unconnected layers to maintain their shape without requiring the support of the previously printed ones.

Analysis of the high-speed video printing process revealed that there is no disturbance in the fluidity of the printing tip, i.e., the tip flows freely allowing writing from layer to layer. We also see that despite the movement that the structure undergoes with the deposition of layers, it always recovers its initial position without fall apart (Figure 4.4 and movie S1).

3.4. 3D printing of complex biological structures

The impression of structures using delicate and soft materials is of growing interest for their potential use in the creation of living tissues [16]. However, one of the major impediments is the fact that it is necessary to create macroscopic structures that allow the normal functioning of the tissues, that is to say that allow the exchange of gases and metabolites [17].

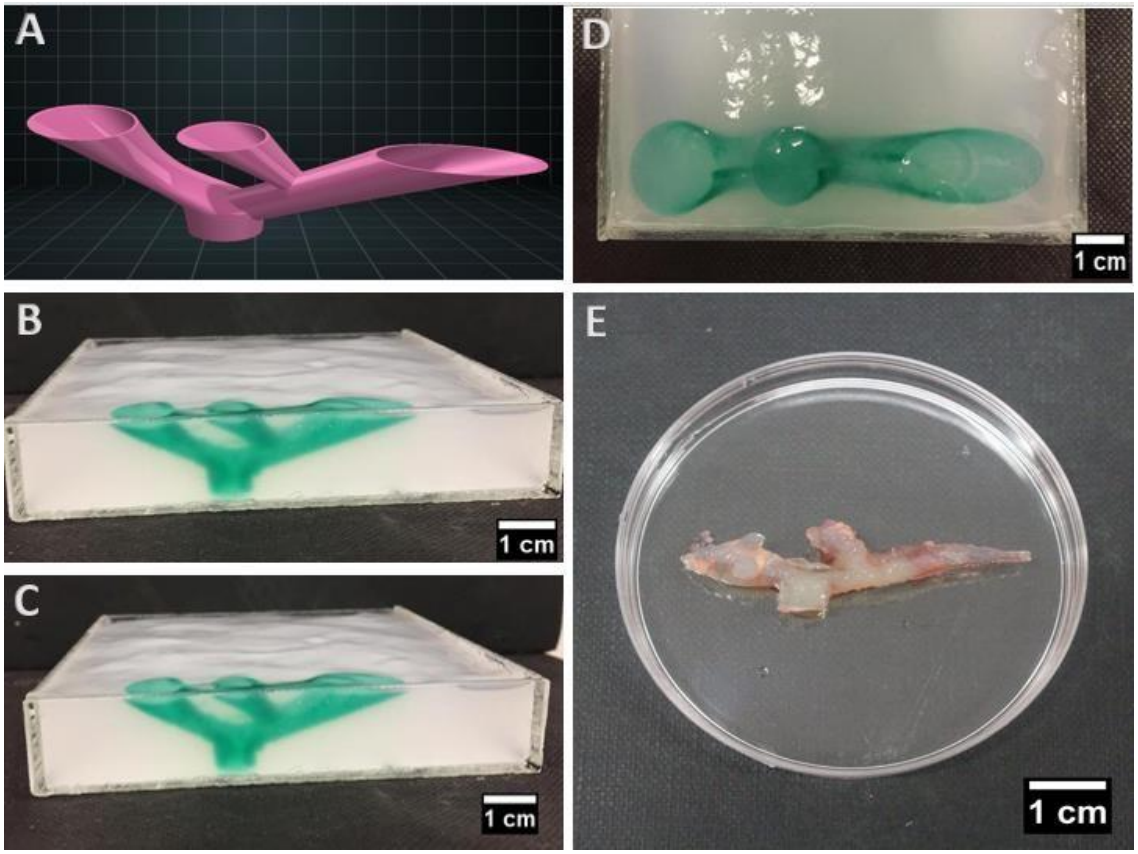

Figure 4.5. Vascular network printing in liquid bath. (A) 3D CAD model of the bifurcation structure; (B) *T*he printed structure immediately printing; (C) The printed structure 24h after printing; (D) Top view of the printed structure; (E) Tubular structure after removing the support bath.

Thus, as evidence that the liquid medium provides excellent stability and accuracy even for such materials and can be applied to tissue engineering, a complex multi-tubular design structure with preservation of shape fidelity is printed inside a bath support. The 3D model is shown in Figure 4.5.A where the bifurcation structure consists of 1 main entrance tube and 3 outlet tubes that mimic the structures found in the human vasculature. The structures printed on the Figure 4.5.B, C and D shows that the printed construction reflects a stable structure with uniform characteristics during and after the entire printing process, respectively. These structures that mimic human arteries demonstrate complex 3D print geometries using liquid hydrogels. The structure after printing was removed from the xanthan gum bath by immersion in a gently swirling water bath. After dispersion of the medium, the artery maintained its complete structural integrity. The thickness of the wall is very thin allowing to see the various layers, however they remain united and cohesive even without any support (Figure 4.5.E). This artery to be feasible for application in tissue engineering, needs to be hollow to allow flow passage. To prove exactly this, we inject water

into it with red dye, confirming that the artery is hollow, allowing passage of the flow and is solid enough to prevent diffusion through the wall (movie S2). Thus, we have shown that this artery, in addition to imitating closely the actual external artery, also does it internally, as it can allow the passage of blood flow.

3.5. Biocompatibility of the support bath

In order to evaluate the biocompatibility of the support bath and its ability to keep cell alive during printing process and in culture medium up to 7 days, live/dead assays were performed. It should also mentioned that 3D bio-printing/plotting techniques for tissue scaffold fabrication have become popular due to their ability to manipulate biomaterial-cell suspensions with a high density of living cells. However, during the bioprinting process the cells are subjected to shear stresses, which can also affect cell viability.

L929 mouse fibroblasts were used in a first screening of the biological performance of the alginate hydrogels. Cells are incorporated in 3ml of culture medium and encapsulated in alginate hydrogels at 3,5% (w/w) were cultured for 7 days and at determined time points, namely 3 and 7 days, analysis to cell viability and proliferation were performed. Figure 4.6 shows that cells are well distributed within the hydrogel, exhibiting high viability at the 3rd and 7th days, showing cell clusters formation at day 7 (figure 4.6).

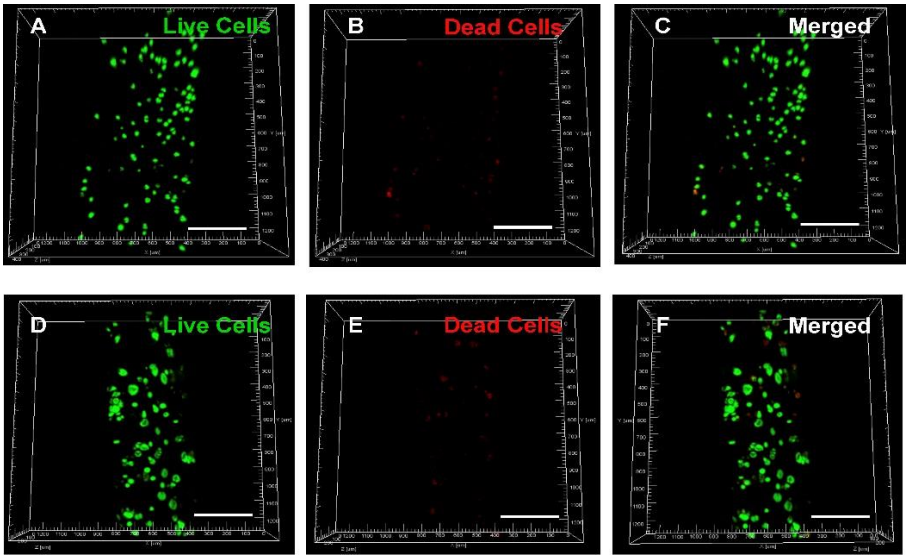

Figure 4.6. Confocal laser scanning microscopy images of L929 mouse fibroblasts encapsulated in the 3D alginate filament after 3 days (A, B and C) and 7 days (D, E, F) of incubation. Fluorescence representative image of the encapsulated living cells (green) in the 3D printed filament (G).

3.6. Fabrication of a perfusable XG-based device

The chemical functionalization of XG with methacrylate moieties was successfully confirmed by NMR spectroscopy (Figure S1, supporting information) with the appearance of vinyl protons at 6.25 and 6.66 ppm. Moreover, the increase intensity of the band around 1720 cm^{-1} in the FTIR-ATR spectra also indicates the presence of the carbon double bonds arise from methacrylate moieties. To evaluate the ability of XG-GMA to form stable hydrogels, a solution of 1.0% XG-GMA was prepared in phosphate-buffered saline containing 0.5% of I2959 photoinitiator. Upon photopolimerization, we obtain a stable 3D hydrogel networks (4.7.A). In this sense, a spiral alginate filament was printed within a 1.0% XG-GMA solution and then exposed to a UV light irradiation for 60 s. In figure 4.7.B is possible to observe the alginate filament hydrogel (the alginate solution was previously labeled with a fluorescence dye) within the XG-GMA hydrogel. This hydrogel system was then emerged in a EDTA in order to liquefied the alginate hydrogel leading to the formation of a perfusable microchannel within the XG-GMA support hydrogel. The perfusion extension was confirmed by injecting a blue dye aqueous solution into the microchannel (Fig 4.7.C). The free movement of the blue dye solution along the spiral microchannel confirms the successfully perfused engineered constructs opening new prospects for biomedical applications.

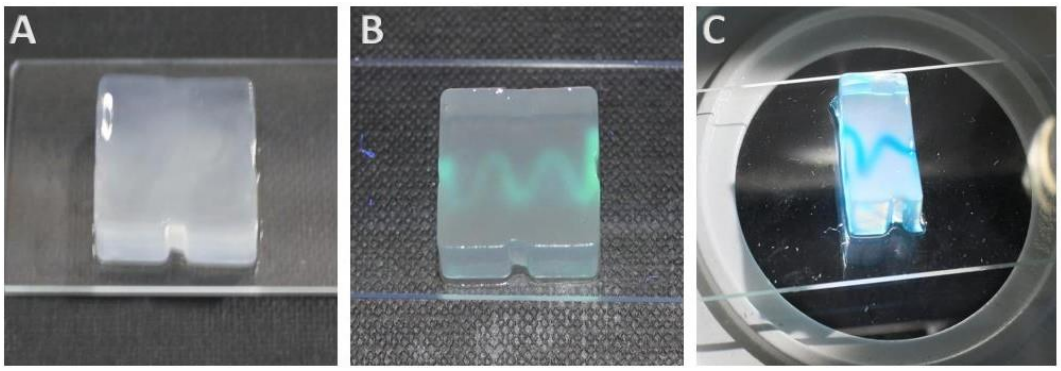

Figure 4.7. A) XG-GMA hydrogel; B) Alginate hydrogel filament within the XG-GMA support hydrogel and C) Blue dye through the microchannel.

4. Conclusions and future perspectives

In conclusion, a novel liquid and hydrogel support bath based on xanthan gum was successfully developed allowing i) to print and remove complex and totally asymmetric hydrogel structures and ii) to fabricate a perfused microchannel device. In particular, we envisioned the possibility to generate more sophisticated microchannel designs, which will be able to recreate specific and peculiar anatomical and physiological features. As future work we suggest the encapsulation of L929 cells within the perfused hydrogel support to evaluate the efficiency in keeping cell alive near the microchannel where the fluid transport of oxygen and metabolite exchange should occur.

5. References

1. Mao, A. S.; Mooney, D. J. Regenerative Medicine: Current Therapies and Future Directions. *Proc. Natl. Acad. Sci. U. S. A.* **2015**, *112* (47), 14452. https://doi.org/10.1073/PNAS.1508520112.

2. Langer, R.; Vacanti, J. P. Tissue Engineering.

3. Murphy, S. V; Atala, A. 3D Bioprinting of Tissues and Organs. *Nat. Biotechnol.* **2014**, *32* (8), 773–785. https://doi.org/10.1038/nbt.2958.

4. Bajaj, P.; Schweller, R. M.; Khademhosseini, A.; West, J. L.; Bashir, R. 3D Biofabrication Strategies for Tissue Engineering and Regenerative Medicine. *Annu. Rev. Biomed. Eng.* **2014**, *16* (1), 247–276. https://doi.org/10.1146/annurev-bioeng-071813-105155.

5. Groll, J.; Boland, T.; Blunk, T.; Burdick, J. A.; Cho, D.-W.; Dalton, P. D.; Derby, B.; Forgacs, G.; Li, Q.; Mironov, V. A.; et al. Biofabrication: Reappraising the Definition of an Evolving Field. *Biofabrication* **2016**, *8* (1), 013001. https://doi.org/10.1088/1758-5090/8/1/013001.

6. Loessner, D.; Meinert, C.; Kaemmerer, E.; Martine, L. C.; Yue, K.; Levett, P. A.; Klein, T. J.; Melchels, F. P. W.; Khademhosseini, A.; Hutmacher, D. W. Functionalization, Preparation and Use of Cell-Laden Gelatin Methacryloyl–based Hydrogels as Modular Tissue Culture Platforms. *Nat. Protoc.* **2016**, *11* (4), 727–746. https://doi.org/10.1038/nprot.2016.037.

7. Tibbitt, M. W.; Anseth, K. S. Hydrogels as Extracellular Matrix Mimics for 3D Cell Culture. *Biotechnol. Bioeng.* **2009**, *103* (4), 655–663. https://doi.org/10.1002/bit.22361.

8. Ladet, S.; David, L.; Domard, A. Multi-Membrane Hydrogels. *Nature* **2008**, *452* (7183), 76–79. https://doi.org/10.1038/nature06619.

9. Li, L.; Yu, F.; Zheng, L.; Wang, R.; Yan, W.; Wang, Z.; Xu, J.; Wu, J.; Shi, D.; Zhu, L.; et al. Natural Hydrogels for Cartilage Regeneration: Modification, Preparation and Application. **2018**. https://doi.org/10.1016/j.jot.2018.09.003.

10. Augst, A. D.; Kong, H. J.; Mooney, D. J. Alginate Hydrogels as Biomaterials. *Macromol. Biosci.* **2006**, *6* (8), 623–633. https://doi.org/10.1002/mabi.200600069.

11. Lee, K. Y.; Mooney, D. J. Alginate: Properties and Biomedical Applications. *Prog. Polym. Sci.* **2012**, *37* (1), 106–126. https://doi.org/10.1016/j.progpolymsci.2011.06.003.

12. Hennink, W. E.; van Nostrum, C. F. Novel Crosslinking Methods to Design Hydrogels. *Adv. Drug Deliv. Rev.* **2012**, *64*, 223–236. https://doi.org/10.1016/j.addr.2012.09.009.

13. Hinton, T. J.; Jallerat, Q.; Palchesko, R. N.; Park, J. H.; Grodzicki, M. S.; Shue, H.-J.; Ramadan, M. H.; Hudson, A. R.; Feinberg, A. W. Three-Dimensional Printing of Complex Biological Structures by Freeform Reversible Embedding of Suspended Hydrogels. *Sci. Adv.* **2015**, *1* (9), e1500758–e1500758. https://doi.org/10.1126/sciadv.1500758.

14. Bhattacharjee, T.; Zehnder, S. M.; Rowe, K. G.; Jain, S.; Nixon, R. M.; Sawyer, W. G.; Angelini, T. E. Writing in the Granular Gel Medium. *Sci. Adv.* **2015**, *1* (8), e1500655–e1500655. https://doi.org/10.1126/sciadv.1500655.

15. Huang, J.; Li, Z.; Hu, Q.; Chen, G.; Ren, Y.; Wu, X.; Ren, J. Bioinspired Anti-Digestive Hydrogels Selected by a Simulated Gut Microfluidic Chip for Closing Gastrointestinal Fistula. **2018**. https://doi.org/10.1016/j.isci.2018.09.011.

16. Muth, J. T.; Vogt, D. M.; Truby, R. L.; Mengüç, Y.; Kolesky, D. B.; Wood, R. J.; Lewis, J. A. Embedded 3D Printing of Strain Sensors within Highly Stretchable Elastomers. *Adv. Mater.* **2014**, *26* (36), 6307–6312. https://doi.org/10.1002/adma.201400334.

17. Miller, J. S.; Stevens, K. R.; Yang, M. T.; Baker, B. M.; Nguyen, D.-H. T.; Cohen, D. M.; Toro, E.; Chen, A. A.; Galie, P. A.; Yu, X.; et al. Rapid Casting of Patterned Vascular Networks for Perfusable Engineered Three-Dimensional Tissues. *Nat. Mater.* **2012**, *11* (9), 768–774. https://doi.org/10.1038/nmat3357.

Supporting information

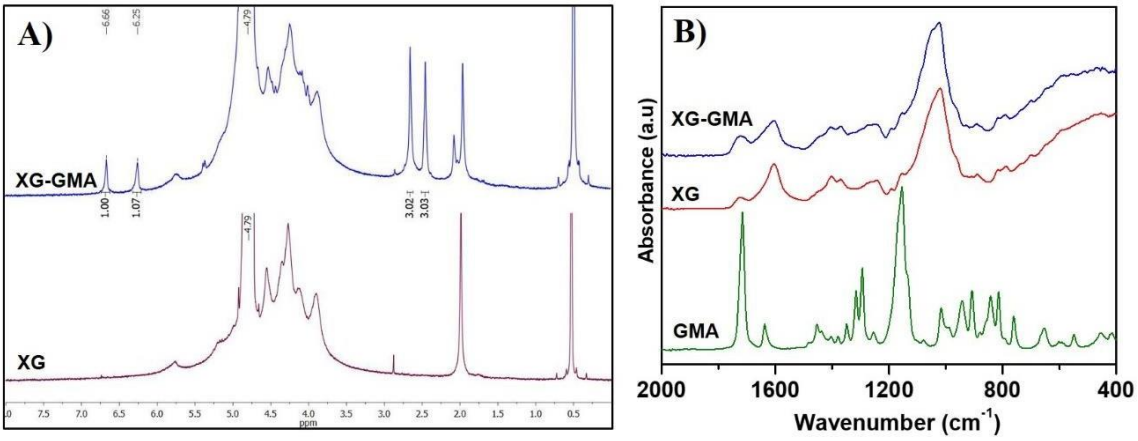

Figure S1. Characterization of synthesized XG-GMA polymer: A) ^{1}H NMR and B) ATR-FTIR spectra.

Supporting Movie Captions

Movie S1.MOV. Proof-of-concept of the true freeform structure.

Movie S2.wmv. Time lapse video of an asymmetric structure being printed. A completely asymmetric structure is imprinted in alginate in the xanthan gum support bath, the alginate has a green dye to aid visualization.

Movie S3.wmv. Perfusion of a printed arterial tree. An arterial tree printed in xanthan gum was removed from the bath and injected with dye to demonstrate manifold structure under flow.

Movie S4.mp4. Free movement of the blue dye solution along the spiral perfusable microchannel.